U.S. Department of Transportation
National Highway Traffic Safety Administration

NHTSA

DOT HS 813 540a

May 2024

Restraint Design for Obese Occupants

Page intentionally left blank.

Suggested APA Format Citation:

Joodaki, H., Gepner, B., & Kerrigan, J. R. (2024, May). *Restraint design for obese occupants* (First of four parts. Report No. DOT HS 813 540a). National Highway Traffic Safety Administration.

The other three parts of this series:

Kerrigan, J. R., Joodaki, H., Sun, Z., & Gepner, B. (2024, May). *Restraint design for obese occupants: Rear-seat simulations* (Second of four parts. Report No. DOT HS 813 540b). National Highway Traffic Safety Administration.

Sun, Z., Kerrigan, J. R., Joodaki, H., & Gepner, B. (2024, May). *Restraint design for obese occupants: Belt pull test simulations error effects modeling* (Third of four parts. Report No. DOT HS 813 540c). National Highway Traffic Safety Administration.

Kerrigan, J. R., Forman, J., Gepner, B., Joodaki, H., & Sun, Z. (2024, May). *Restraint design for obese occupants: Obese GHBMC model modifications* (Fourth of four parts. Report No. DOT HS 813 540d). National Highway Traffic Safety Administration.

Page intentionally left blank.

Technical Report Documentation Page

1. Report No.	2. Government Accession No.	3. Recipient's Catalog No.
DOT HS 813 540a		

4. Title and Subtitle	5. Report Date
Restraint Design for Obese Occupants (First of four parts)	May 2024
	6. Performing Organization Code
7. Authors Hamed Joodaki, Bronek Gepner, Jason R. Kerrigan	**8. Performing Organization Report No.**
9. Performing Organization Name and Address University of Virginia Center for Applied Biomechanics 4040 Lewis and Clark Drive Charlottesville, VA 22911	**10. Work Unit No. (TRAIS)** **11. Contract or Grant No.** DTNH2215D00022
12. Sponsoring Agency Name and Address National Highway Traffic Safety Administration 1200 New Jersey Avenue SE Washington, DC 20590	**13. Type of Report and Period Covered** **14. Sponsoring Agency Code**

15. Supplementary Notes

16. Abstract

This study drew conclusions by conducting research in five different parts: the effect of obesity on the risk of injury to different body regions; the most frequent injuries of occupants with and without obesity and the potential injury mechanism of the most frequent injuries of occupants with obesity; quantified comparison of the response of a Global Human Body Modeling Consortium obesity model to an obese postmortem human surrogate; the effect of restraint system parameters on the obese and non-obese human body model (HBM) responses, including the HBM kinematics and the values of different injury metrics; assessment of the prediction ability of several advanced machine learning techniques for restraint design parametric simulations; demonstrating leveraging machine learning to predict the response of simulations with HBMs to avoid over-fitting and under-fitting; comparison of the parameters defining the optimized restraint system for an obese HBM, non-obese HBM, and both HBMs concurrently. This is the first of four parts of this study.

17. Key Words	18. Distribution Statement
human body model, post morten human surrogate, sled test, seat belt, Global Human Body Modeling Consortium, GHBMC, obesity	This document is available to the public from the DOT, BTS, National Transportation Library, Repository & Open Science Access Portal, https://rosap.ntl.bts.gov.

19. Security Classif. (of this report)	20. Security Classif. (of this page)	21. No. of Pages	22. Price
Unclassified	Unclassified	77	

Form DOT F 1700.7 (8-72) Reproduction of completed page

Page intentionally left blank.

Table of Contents

List of Figures

List of Tables

Page intentionally left blank.

Executive Summary

Several epidemiology studies have shown that obesity, an epidemic, is associated with an increased risk of injury and fatality in motor vehicle crashes (MVC). Hence, investigating strategies for increased safety of occupants with obesity would improve public health. The research question answered in this study was whether an optimized restraint system for an occupant with obese anthropometry would be different than that for an occupant with a normal body mass index (BMI).

This study had five different parts. In the first part, a field data analysis was performed to compare the risk of injury to different body regions amongst different BMI categories and to identify the most common injuries of occupants with obesity. In the second part, the performance of an available obese human body model (HBM) (BMI=35) was assessed through comparing its behavior to an obese postmortem human surrogate (PMHS) with similar BMI and height, under the same conditions. In the third part, parametric simulations were performed with obese (BMI=35) and normal (BMI=25) HBMs and 14 different restraint parameters. Afterwards, statistical, and biomechanical analyses were conducted on the parametric simulation results. In the fourth part, machine learning was leveraged to develop metamodels of the simulation results. In the fifth part, the genetic algorithm operated on the metamodels to identify the optimal solutions. Optimization was performed for: (1) obese HBM individually; (2) non-obese HBM individually; and (3) obese and non-obese HBMs concurrently.

Field data analysis showed that the increased injury risk of occupants with obesity, observed in previous field data studies, stems from increased risk of injury to the extremities and spine. HBM evaluation showed that the obese replicated HBM represented some key biomechanical characteristics that are potentially challenging to design an effective restraints system. Specifically, a relatively large lower extremity excursion and lower tendency to pitch forward when compared to occupants with normal BMI. Statistical analyses on the parametric simulations elucidated the effects of different restraint parameters on the responses of obese and non-obese HBMs. Efforts to leverage machine learning for developing metamodels of the simulations showed that optimizing hyperparameters of the metamodels can substantially increase accuracy. The optimization results revealed that the general strategy for occupants with and without obesity should be similar. The occupant's kinetic energy should be partially overcome by the force of a seat belt with a low load-limiter level which lets the occupant use the available space for forward motion, and the remainder of this energy should be dissipated by other restraints, including tuned air bags and a collapsible steering column. However, The optimized restraint system for the occupant with obesity included an under-the-seat air bag (USAB), which made the kinematics of this occupant more favorable throughout the crash event and mitigated the risk of the lower extremity and spinal injuries. Also, the optimized restraint for both occupants included an inflatable seat belt (ISB), which decreased the risk of thoracic injury.

Page intentionally left blank.

Summary of Findings

Field Data Analysis

- The increased risk of injury observed for occupants with obesity in the previous studies can be attributed to their increased risk of injury to the extremities and spine. This can be explained by their large forward motion during the crash due to increased body mass, which results in increased kinetic energy. Additionally, thick adipose tissue results in delayed engagement of the lap belt with the bony structure of the pelvis. These factors cause decreased torso flexion and consequently, increased compression force to the spine, which increases the risk of spinal injuries.
- After adjusting for other variables, the risks of spinal, thoracic, and extremities injuries were found to be affected by BMI class.
- Seven out of the 10 most common injuries sustained by occupants with obesity were lower extremity injuries, with talus fractures being the most common.
- Direct loading through the plantar surface of the foot by the vehicle toe pan was found to be a likely cause of many of those injuries based on Crash Injury Research and Engineering Network (CIREN) cases.

HBM Evaluation

- The obese HBM captures the effects of large body mass and delayed lap belt engagement with the pelvis, similarly to the obese PMHS. These characteristics are critical for front-seat frontal impact simulations.

Parametric Simulations and Statistical Analysis

- The HBMs captured some key biomechanical differences between occupants with and without obesity, including greater lower extremity excursion and increased lower extremity and spinal injury metric values for obese HBM compared to non-obese.
- The general strategies for increasing safety of the non-obese HBM have no compelling counter-effect for the obese HBM.
- However, obesity resulted in a difference in the value of injury metrics across a range of parameters.
- It was hypothesized that the key to increasing the safety of occupants with obesity is to mitigate their lower extremity excursion, which would not only decrease the risk of having an injurious impact with the vehicle interior but also make the occupant's torso pitch forward, resulting in a favorable posture for air bag deployment and decreased risk of spinal injuries.
- The findings suggested ideas with a focus on arresting lower extremity excursion can be considered to increase the safety of occupants with obesity when designing a restraint system. For example, the USAB reduced the lower extremity excursion and injury metric values and thus might be useful for protecting occupants with obesity from suffering an increased risk of lower extremity injury for non-obese occupants. Also, the ISB can be an effective countermeasure to decrease the occupant's chest and neck injuries.

- Modifying restraint parameters, occasionally decreased the risk of injury to a body region but increased the risk to another region. A comprehensive restraint system optimization with a range of anthropometries is necessary to find the most favorable set of restraint parameters.

Metamodel Development

- Machine learning techniques showed a higher prediction accuracy compared to linear ordinary least squares (OLS) regression techniques. In addition, if linear OLS is used for the optimization, the optimization process would converge in the boundaries. Hence, machine learning techniques were more suitable than the linear OLS for developing metamodels, which would be used for restraint system optimization.
- The optimization algorithm would operate on the metamodel to identify the optimal region. Therefore, the metamodel should be able to capture the correlation patterns between the design parameters and the objective function. As the shape of response surface approximated by the metamodels is dependent on the value of their hyperparameters, optimizing hyperparameters is crucial for the metamodels that are developed for restraint system optimization. Solely selecting some random hyperparameters without optimization and then training the metamodel might result in failing to find the actual optimized design.

Restraint System Optimization

- Overall, while the general strategy for restraining both obese and non-obese HBMs was similar, the optimization results suggested considering the USAB as an additional countermeasure to better protect the obese HBM.
- The general restraint strategy for both occupants should be using a low load limiter (LL) level to partially overcome the occupant's kinetic energy through a low force applied to the chest and a large displacement (work = force × displacement) and dissipating the remainder of this energy using other restraints including tuned driver air bags and a collapsible steering column, which would apply the load to a wide area of the body.
- The optimized restraint for both HBMs included the inflatable seat belt, as it mitigated the risk of thoracic injury by distributing the force into a wider area compared to the regular seat belt.
- The optimized restraint for the obese HBM included the USAB, which made the occupant's kinematics more favorable by decreasing the lower extremity excursion and increasing the occupant's tendency to pitch forward and mitigated its lower extremity and spinal injuries. The USAB can be an effective countermeasure for increased safety of occupants with obesity.
- A vehicle system that can measure the occupant's weight using seat sensors and estimate the occupant's height from the seat position could potentially help to determine if the countermeasures, which are effective for occupants with obesity, including the USAB, should be activated during a crash.
- Further investigations, including experimental tests, are necessary to confirm these findings.

Introduction

This section provides background research and motivations for this report, concluding with a parts overview.

Study Objective

In 2015 the World Health Organization reported that worldwide motor vehicle crash fatalities had plateaued at about 1.25 million in 2013. Further, some 50 million people were injured in that period. Designing effective countermeasures is the chief approach to protecting the occupants if an MVC occurs, and continuing efforts are made to increase the occupant safety during a vehicle crash. It is estimated that more than 613,000 lives were saved by vehicle safety technologies and associated Federal Motor Vehicle Safety Standards from 1960 to 2012 in the United States (Kahane, 2015). Investigating methods for maximizing the safety of occupants with different characteristics can contribute to saving even more lives. This study was a step toward that goal. The objective of this study was to design an optimized restraint for an occupant with obesity.

There were two important reasons to study restraint strategies for the obese. First, a substantial proportion of the U.S. population is obese. Second, several field data studies have shown that obesity is associated with increased risk of fatality and injury in MVCs.

Safety of Occupants with Obesity in Motor Vehicle Collisions

Obesity has become an epidemic in the United States. From 1988–1989 to 2003–2004, the mean waist circumference of U.S. adults increased continuously (Li et al., 2007). About 34.9 and 14.5 percent of the U.S. adult population were reported to be obese (BMI≥30 kg/m^2) and severely obese (BMI≥35 kg/m^2) respectively in 2011–2012 (Ogden et al., 2014). Similarly, the rate of obesity has been increasing worldwide. A study on 19.2 million adults from 186 countries showed that the proportion of obese males increased from 3.2 percent in 1954 to 10.8 percent in 2014 (NCD Risk Factor Collaboration, 2016) while the proportion of obese females increased from 6.4 to 14.9 percent, over in the same time span.

Obesity is associated with an increased risk of fatality in MVCs. Viano et al. (2008) studied the risk of fatality for front-seat occupants in MVCs using the Crashworthiness Data System (CDS) of the National Automotive Sampling System (NASS) and found out that for a given stature, the occupants with a BMI of 30–35 kg/m^2 are 97 percent more likely to die in MVCs than the occupants with BMI of 18–25 kg/m^2. Similarly, Zhu et al. (2006) found that the risk of death due to MVCs increases at both ends of BMI (BMI<20 kg/m^2 and BMI≥35 kg/m^2) among men. Mock et al. (2002) observed an increased risk of death in MVCs with increased weight and reported the odds ratio for death to be 1.013 for each kilogram increase in body weight.

Obesity also increases the risk of injury in MVCs. Viano et al. (2008) reported occupants with BMI of 30 to 35 kg/m^2 to have 17 percent higher risk of Maximum Abbreviated Injury Scale 3+ than normal BMI occupants. After adjusting for the crash speed, Ma et al. (2011) showed that male drivers with obesity have an increased risk of non-fatal injury compared to other male drivers. They also showed that this risk increases with the severity of injury. Mock et al. (2002) determined an odds ratio of 1.008 for sustaining an injury with Injury Severity Score (ISS) ≥ 9 for each kilogram increase in body mass. Finkelstein et al. (2007) found that the occupants with normal BMI (20 kg/m^2 ≤BMI < 25 kg/m^2) have the lowest risk of sustaining injury in MVCs amongst all BMI categories. On the other hand, Class I and Class III obesity were at the highest risk of injury in MVCs (odds ratio of 1.24 with respect to the normal BMI occupants).

To shed light on the injury mechanism and potential reasons for such observations, Forman et al. (2009) performed experimental frontal impact sled tests with obese and non-obese PMHS. It was observed that the obese PMHS tended to experience a larger forward motion of lower extremity compared to non-obese. In addition, in contrast to non-obese PMHS, the torso angle of obese PMHS did not pitch forward which created an undesired posture for air bag deployment. Also, the obese PMHS tended to submarine, defined as the lap belt moving up over the pelvis into the abdomen. Besides that, a volunteer study showed that the occupants with obesity tend to wear their lap belt higher, with respect to the pelvis, compared to other occupants (Reed et al., 2012). Such behavior would also increase the risk of submarining (Kim et al., 2015).

The kinematic differences observed in Forman et al. (2009) could be attributed to three main reasons. First, most of the kinetic energy must be overcome by the work (work-energy theorem) that the seat belt does on the occupant to constrain him/her. The obese PMHS had a bigger body mass and consequently larger kinetic energy than the non-obese PMHS. Hence, with the same amount of seat belt force, a larger displacement was required to achieve more work (work = force × displacement). That is a reason why the obese PMHS stopped moving relative to the vehicle after a larger displacement than the non-obese PMHS. Second, the lap belt force was initially spent on the deformation of the obese PMHS' thick adipose tissue, which resulted in the delayed engagement of the belt with the bony structure of the pelvis. This caused a delayed forward torso flexion, which resulted in lower overall torso angle change. The delayed engagement and soft tissue deformation also contributed to the PMHS' large forward motion. Third, lap belt loading to the adipose tissue surrounding the pelvis resulted in a high compressive load and high shear deformation of the adipose tissue. The shear deformation allowed the lap belt to move upward and over the pelvis resulting in submarining (Forman et al., 2009; Kent et al., 2010).

These studies showed that current restraint systems are not as effective for occupants with obesity as they are for non-obese occupants. Also, considering that the main target of vehicle safety regulations is a mid-sized occupant (BMI=25 kg/m^2, height=175 cm), the findings raised the question of whether the restraint approach for occupants with obesity should be different than that for mid-sized occupants. Since occupants with obesity make up a considerable proportion of the population in the United States and elsewhere (Ogden et al., 2014; NCD Risk Factor Collaboration, 2016), investigating the methods to protect them in vehicle crashes could help address this major public health problem. The main goal of this project was to investigate whether an optimized restraint system for occupants with obesity would be different than that for midsize occupants, and how the restraint system should be modified to increase the safety of occupants with obesity.

Obese Human Body Models

To better understand details associated with injury risks of occupants with obesity in vehicle crashes, and to begin to address these risks through restraint system or other countermeasure designs, it is necessary to have biofidelic surrogates which can replicate the response of occupants with obesity in MVCs. To address this need, some obese HBMs have been developed by morphing the external body contour and exterior skeleton geometry of baseline (midsize male) HBMs. Such obese versions of the Total Human Model for Safety were evaluated in detail through previous studies (Shi et al., 2015; Zhang et al., 2017; Kitagawa et al., 2017). Additionally, Hu et al. (2016) performed a similar methodology to develop obese versions of the Global Human Body Modeling Consortium (GHBMC) M50-O model by adjusting BMI, height, and age. In this project, an obese HBM, which was developed by morphing the detailed GHBMC midsize model, was evaluated and then used for restraint system optimization.

Page intentionally left blank.

Part 1: Field Data Analysis

Paper 1, Joodaki et al. (2019), further details the goal, methods, results, and conclusions of the study.

Motivation and Goal

The goals of this part were to determine:

- The risk of injury to different body regions amongst subjects in different BMI categories,
- The most frequent injuries experienced by occupants with obesity, and
- The potential injury mechanism of those injuries.

This information was necessary to develop effective countermeasures for occupants with obesity.

Methods

Sampled cases (n = 13,470) representing ~4.7 million adult occupants involved in frontal crashes from 2000 to 2015 were selected from NHTSA's NASS-CDS database (Table 1). A retrospective cohort study was performed to study the effect of BMI on the risk of injury to different body regions and to identify the most frequent injuries to occupants with different BMIs. Besides, in-depth crash analysis cases from the CIREN database were studied to elucidate the source of the most common injuries to occupants with obesity.

Table 1. Characteristics of the sample

	Population (unweighted)	Population (weighted)	AIS2+ Injured Population (unweighted)	AIS2+ Injured Population (weighted)	Female Proportion (%) (CI)	Vehicle Weight (kg)(CI)	Model Year(CI)
All	13,470	4,663,682	3,175	468,247	50 (48,53)	632(624,640)	2002.44 (2002.22,2002.67)
Obese	2,933	868,937	850	130,586	50 (45,54)	641(618,664)	2003.07 (2002.59,2003.56)
Non-Obese	10,537	3,794,745	2,325	337,655	50 (47,53)	634(621,639)	2002.3 (2002.04,2002.55)
Underweight	1,167	418,376	246	35,973	78 (72,84)	611(581,642)	2002.09 (2001.43,2002.74)
Normal	4,983	1,838,796	1,061	155,922	54 (50,58)	630(617,642)	2002.07 (2001.67,2002.47)
Overweight	4,387	1,537,573	1,018	145,760	39 (33,44)	637(623,651)	2002.62 (2002.26,2002.98)
Obese1	1,846	576,683	478	68,368	47 (41,52)	642(611,674)	2002.92 (2002.32,2003.52)
Obese2	6,76	197,871	210	41,564	53 (42,63)	645(606,682)	2003.66 (2002.54,2004.78)
Obese3	411	94,383	162	20,655	62 (52,71)	625(608,642)	2002.78 (2001.94,2003.63)
p-value					<0.0001†	0.004*	<0.0001*

						Vehicle Type			
	Driver Position (%)(CI)	**Delta V (kph) (CI)**	**Height (cm) (CI)**	**Weight (kg) (CI)**	**Age(CI)**	**Passenger Car (%)(CI)**	**Truck (%)(CI)**	**Van (%)(CI)**	**Utility (%)(CI)**
All	86 (85, 88)	23.58 (23.10, 24.05)	171.47 (1797, 171.98)	76.9 (76.0, 77.8)	37.07 (36.25, 37.89)	70 (67, 72)	10 (8, 12)	6 (5, 7)	14 (13, 17)

Obese	87 (84, 9)	24.01 (23.02, 25.01)	1711 (168.97, 171.24)	107 (99.0, 102.5)	449 (39.04, 41.93)	68 (63, 72)	11 (7, 14)	6 (5, 8)	15 (12, 18)
Non-Obese	86 (84, 88)	23.47 (22.93, 24.00)	171.79 (171.23, 172.34)	71.5 (75, 72.4)	36.28 (35.34, 37.23)	70 (67, 73)	10 (7, 12)	5 (5, 6)	15 (12, 17)
Underweight	85 (82, 89)	23.82 (22.73, 24.91)	168.94 (167.82, 176)	53.6 (52.8, 54.4)	31.02 (28.53, 33.52)	74 (68, 81)	8 (1, 14)	4 (2, 6)	14 (10, 17)
Normal	84 (81, 87)	23.43 (22.66, 24.21)	171.52 (1782, 172.22)	66.8 (66.2, 67.5)	34.90 (33.58, 36.22)	74 (71, 77)	7 (5, 8)	5 (4, 7)	14 (11, 17)
Overweight	89 (87, 91)	23.40 (22.50, 24.30)	172.88 (171.88, 173.88)	81.9 (85, 83.2)	39.38 (37.67, 41.08)	64 (58, 70)	14 (9, 20)	6 (5, 7)	16 (11, 21)
Obese1	86 (81, 90)	23.93 (22.66, 25.2)	1730 (168.76, 171.83)	93.6 (91.7, 95.4)	477 (38.85, 42.68)	70 (65, 75)	10 (7, 13)	5 (3, 6)	15 (11, 19)
Obese2	92 (9, 95)	23.60 (21.60, 25.59)	1764 (168.80, 172.48)	108.7 (105.7, 111.8)	39.31 (36.71, 41.90)	60 (48, 71)	17 (5, 29)	10 (3, 16)	13 (8, 19)
Obese3	87 (82, 92)	25.44 (23.21, 27.67)	167.84 (165.36, 1732)	127.6 (123.9, 131.3)	41.23 (38.58, 43.89)	68 (58, 77)	5 (2, 7)	10 (5, 15)	17 (10, 26)
p-value	<0.0001†	0.057*	<0.0001*	<0.0001*	<0.0001*	<0.0001†			

*: ANOVA associated p-value for quantitative variables which had an approximately normal distribution
†: Chi-squared test associated p-value for categorical variables
Values are reported in form of “mean (CI)”

Results

- Occupants with obesity experienced a higher risk of upper extremity, lower extremity, and spine injuries than normal BMI occupants (Table 2).
- After adjusting for other variables, the risks of spinal, thoracic, and extremities injuries were found to be affected by the BMI class (Table 3).
- Seven out of the 10 most common injuries sustained by occupants with obesity were lower extremity injuries, and talus fractures were the most common overall (Table 4).
- Sternum fracture was the most frequent injury of non-obese occupants (Table 5).
- Direct loading through the plantar surface of the foot by the vehicle toe pan was found to be a likely cause of many lower extremity injuries based on CIREN cases (Table 6).

Table 2. Risk (%) of AIS2+ injuries to different body regions for different BMI groups in frontal crashes

	All Injuries (CI)	Head (CI)	Face (CI)	Neck (CI)	Thorax (CI)
All Occupants	10.04 (8.88, 11.20)	1.89 (1.55, 2.24)	0.21 (0.15, 0.27)	0.02 (0.01, 0.03)	2.36 (1.89, 2.83)
Obese	15.03 (11.34, 18.71)	1.97 (1.37, 2.57)	0.21 (0.06, 0.36)	0.03 (0, 0.06)	2.29 (1.73, 2.85)
Non-Obese	8.90 (7.79, 10.01)	1.88 (1.48, 2.28)	0.21 (0.14, 0.27)	0.02 (0, 0.03)	2.38 (1.81, 2.94)
Underweight	8.60 (6.36, 10.84)	2.21 (1.29, 3.14)	0.18 (0.02, 0.34)	0 (0, 0.01)	2.16 (0.96, 3.37)
Normal	8.48 (6.89, 10.07)	1.55 (1.17, 1.92)	0.23 (0.13, 0.34)	0.02 (0, 0.04)	2.46 (1.61, 3.31)
Overweight	9.48 (7.59, 11.37)	2.18 (1.34, 3.02)	0.18 (0.08, 0.28)	0.02 (0, 0.03)	2.34 (1.44, 3.23)
Obese I	11.86 (8.67, 15.04)	1.84 (1.15, 2.52)	0.15 (0.03, 0.26)	0.03 (0, 0.06)	1.95 (1.35, 2.55)
Obese II	21.01 (9.19, 32.82)	2.17 (0.62, 3.73)	0.10 (0, 0.21)	0.04 (0, 0.12)	2.19 (1.18, 3.20)
Obese III	21.88 (13.23, 30.54)	2.38 (0.84, 3.91)	0.83 (0, 1.98)	0.01 (0, 0.03)	4.56 (1.68, 7.44)
Injured Population: Unweighted (weighted)	3175 (468241)	792 (883756)	150 (9671)	20 (819)	934/110119.1
Chi-Square Test p-Value	<0.0001*	0.246	0.293	0.994	0.190
	Abdomen (CI)	**Spine (CI)**	**Upper Extremity (CI)**	**Lower Extremity (CI)**	
All Occupants	0.61 (0.40, 0.81)	1.17 (0.86, 1.48)	3.26 (2.67, 3.86)	4.19 (3.36, 5.01)	
Obese	0.64 (0.41, 0.87)	1.53 (0.79, 2.27)	4.78 (2.92, 6.65)	8.37 (5.08, 11.66)	
Non-Obese	0.60 (0.35, 0.85)	1.09 (0.75, 1.43)	2.91 (2.33, 3.50)	3.23 (2.58, 3.87)	
Underweight	0.62 (0.13, 1.11)	0.99 (0.49, 1.49)	2.45 (1.22, 3.69)	3.44 (2.12, 4.76)	
Normal	0.70 (0.22, 1.19)	0.94 (0.48, 1.39)	2.51 (1.85, 3.18)	3.17 (2.08, 4.27)	
Overweight	0.46 (0.30, 0.63)	1.30 (0.67, 1.92)	3.52 (2.35, 4.69)	3.24 (2.40, 4.07)	
Obese I	0.56 (0.30, 0.81)	0.86 (0.48, 1.25)	4.39 (2.06, 6.72)	5.93 (3.81, 8.05)	
Obese II	0.66 (0.15, 1.16)	1.94 (0.31, 3.56)	6.92 (2.35, 11.48)	12.72 (0.75, 24.68)	
Obese III	1.13 (0.17, 2.09)	4.72 (0, 9.97)	2.70 (1.35, 4.04)	14.17 (6.56, 21.77)	

Injured Population: Unweighted (weighted)	384 (28229)	504 (54532)	1061 (152126)	1626 (195260)	
Chi-Square Test p-Value	0.600	<0.0001*	<0.0001*	<0.0001*	
CI: 95% confidence interval *: Significant difference (p-value <0.05) among different BMI groups (underweight, normal, overweight, obese I-III) Values are reported in form of "mean (CI)"					

Table 3. Parameter estimates and standard error from multivariate logistic regressions of AIS 2+ risk of injuries to different body regions in frontal crashes

		Overall Injury		Head		Thoracic		Abdominal	
		Estimate	**SE**	**Estimate**	**SE**	**Estimate**	**SE**	**Estimate**	**SE**
Intercept		-8.563	1.992	-3.639*	1.994	-12.218	3.115	-7.402	2.701
Age		0.025*	0.004	0.007	0.005	0.067*	0.007	0.025*	0.007
Female (vs. male)		0.971*	0.247	0.124	0.225	0.586	0.305	-0.226	0.408
Delta V (kph)		0.075*	0.006	0.062*	0.006	0.087*	0.007	0.075*	0.006
Vehicle Type	Truck	0.371	0.410	-0.645*	0.288	-0.266	0.336	0.047	0.384
(vs. passenger)	Van	-0.533*	0.221	-0.524	0.505	-0.744*	0.373	-0.616	0.507
	Utility	-0.026	0.223	0.025	0.234	-0.317	0.251	0.317	0.379
Passenger Position (vs. driver)		0.412	0.257	-0.285	0.264	0.677*	0.308	0.721	0.402
BMI Category (vs. normal)	Underweight	-0.107	0.232	0.454	0.297	-0.088	0.566	0.055	0.543
	Overweight	0.013	0.168	-0.041	0.269	-0.274	0.301	-0.294	0.359
	Obese I	0.264	0.251	-0.121	0.308	-0.642*	0.264	-0.425	0.448
	Obese II	1.234*	0.448	0.161	0.535	-0.395	0.416	0.423	0.574
	Obese III	0.860*	0.332	0.311	0.446	0.766	0.503	0.518	0.713
Height (cm)		0.015	0.011	-0.015	0.011	0.015	0.016	-0.007	0.015
Model Year-2002		0.000	0.016	0.019	0.022	0.049*	0.022	-0.015	0.034
		Spine		**Upper Extremity**		**Lower Extremity**			
		Estimate	**SE**	**Estimate**	**SE**	**Estimate**	**SE**		
Intercept		-4.508	2.202	-10.193*	2.321	-11.465*	2.899		

Age		0.041*	0.008	0.022*	0.004	0.010	0.007		
Female (vs. male)		0.28	0.306	0.935*	0.248	1.290*	0.384		
Delta V V (kph)		0.077*	0.006	0.059*	0.008	0.073*	0.006		
Vehicle Type	Truck	0.568	0.446	-0.120	0.343	0.715	0.556		
(vs. passenger)	Van	-0.395	0.38	-0.196	0.282	-0.450	0.317		
	Utility	0.056	0.305	0.143	0.402	0.170	0.24		
Passenger Position (vs. driver)		0.510	0.283	0.270	0.391	0.178	0.432		
BMI Category (vs. normal)	Underweight	0.451	0.415	-0.351	0.320	-0.272	0.341		
	Overweight	0.608	0.39	0.287	0.242	-0.083	0.232		
	Obese I	-0.452	0.425	0.457	0.404	0.64*	0.318		
	Obese II	0.901*	0.43	1.129*	0.419	1.717*	0.520		
	Obese III	0.496	0.426	-0.201	0.367	1.575*	0.425		
Height (cm)		-0.029*	0.013	0.021	0.013	0.029	0.015		
Model Year-2002		0.072*	0.024	0.016	0.028	-0.083*	0.018		

SE: Standard error
*: Statistically significant (p-value<0.05)
Values are with respect to the risk of injury as a unit interval ([0,1], not percentage)

Table 4. Risk of most observed injuries of occupants with obesity for obese and non-obese BMI groups in frontal crashes

AIS Code	All Occupants (%, CI)	Obese (%, CI)	Non-Obese (%, CI)	p-Value	Description
853200.2	0.58 (0, 1.17)	2.52 (0, 5.58)	0.14 (0.10, 0.18)	<0.0001*	Talus fracture
853414.2	0.43 (0, 0.99)	1.79 (0, 4.75)	0.12 (0.07, 0.18)	<0.0001*	Tibia fracture medial malleolus open/displaced/comminuted
852200.2	0.65 (0.34, 0.95)	1.77 (0.34, 3.21)	0.39 (0.22, 0.55)	<0.0001*	Metatarsal or tarsal fracture
752002.	1.06 (0.60, 1.51)	1.53 (0.04, 3.01)	0.95 (0.51, 1.39)	0.010*	Carpus or metacarpus fracture
852400.2	0.61 (0.34, 0.87)	1.52 (0.29, 2.76)	0.40 (0.24, 0.56)	<0.0001*	Patella fracture
752800.2	0.44 (0.22, 0.66)	1.33 (0.28, 2.39)	0.24 (0.12, 0.36)	<0.0001*	Radius fracture NFS with or without styloid process including Colles
850826.2	0.74 (0.32, 1.16)	1.07 (0.44, 1.71)	0.66 (0.17, 1.15)	0.028*	Knee sprain
851606.2	0.38 (0.29, 0.48)	0.67 (0.42, 0.93)	0.31 (0.22, 0.41)	0.008*	Fibula fracture; any type but NFS as to site; head, neck, shaft
450220.2	0.45 (0.24, 0.67)	0.62 (0.27, 0.96)	0.41 (0.16, 0.66)	0.164	Rib cage fracture 2–3 ribs any location (OIS Grade I, II or III)
450230.3	0.38 (0.25, 0.51)	0.52 (0.30, 0.74)	0.35 (0.20, 0.50)	0.204	Rib cage fracture >3 ribs on one side and <=3 ribs on the other side

CI: 95% confidence interval
p-value: Chi-squared test associated p-value
*: Statistically significant (p-value<0.05)
Values are reported in form of "mean (CI)"

Table 5. Risk of most observed injuries of non-obese occupants for obese and non-obese BMI groups in frontal crashes

AIS Code	All Occupants (%, CI)	Obese (%, CI)	Non-Obese (%, CI)	p-Value	Description
450804.2	0.94 (0.57, 1.32)	0.45 (0.29, 0.61)	1.06 (0.60, 1.51)	0.004*	Sternum NFS; fracture (OIS Grade II or III)
752002.2	1.06 (0.6, 1.51)	1.53 (0.04, 3.01)	0.95 (0.51, 1.39)	0.010*	Carpus or metacarpus NFS; fracture
850826.2	0.74 (0.32, 1.16)	1.07 (0.44, 1.71)	0.66 (0.17, 1.15)	0.002*	Knee sprain
752200.2	0.54 (0.33, 0.75)	0.35 (0.16, 0.55)	0.58 (0.32, 0.84)	0.159	Clavicle fracture (Grade I or II)
160406.2	0.44 (0.24, 0.64)	0.44 (0.21, 0.66)	0.44 (0.20, 0.69)	0.957	Head (cranium and brain); Awake post resuscitation or on initial observation at scene (GCS 15) NFS; prior unconsciousness, but length of time NFS with neurological deficit
450220.2	0.45 (0.24, 0.67)	0.62 (0.27, 0.96)	0.41 (0.16, 0.66)	0.164	Rib cage fracture 2-3 ribs any location (OIS Grade I, II or III)
852400.2	0.61 (0.34, 0.87)	1.52 (0.29, 2.76)	0.4 (0.24, 0.56)	<0.0001*	Patella fracture
161000.2	0.41 (0.21, 0.61)	0.48 (0.12, 0.85)	0.39 (0.16, 0.62)	0.508	Awake post resuscitation on admission or initial observation at scene (GCS 15) prior unconsciousness.
852200.2	0.65 (0.34, 0.95)	1.77 (0.34, 3.21)	0.39 (0.22, 0.55)	<0.0001*	Metatarsal or tarsal fracture
752802.2	0.35 (0.19, 0.51)	0.30 (0.15, 0.45)	0.36 (0.17, 0.55)	0.621	Radius fracture NFS with or without styloid process including Colles; closed

CI: 95% confidence interval
p-value: associated Chi-squared test p-value
*: statistically significant (p-value<0.05)
Values are reported in form of “mean (CI)”

Table 6. A list of some frontal crash CIREN cases with a large BMI who were belted and experienced the common lower extremity injuries of occupants with obesity

CIREN ID	BMI (kg/m²)	DV (kph) ‡	D/P§	F/M#	853200.2*	853414.2*	852200.2*	852400.2*	850826.2*	851606.2*	Talus Injury Source ^ ǂ	Knee Injury Source °	Talus Fracture Location‡	TP/ IP Intrusion°
109574	41	68	P	M	Y	N	Y	N	N	N	FLR	-	Un	TP & IP
120305	57	46	p	F	Y	N	N	N	N	N	FLR	-	Neck and body	IP
164689	54	54	D	F	Y	N	N	N	N	N	FLR	-	Dome	None
160128189	32	57	D	M	Y	N	Y	Y	N	N	FLR	IP	Un	TP
160132288	29	68	D	M	Y	N	N	N	N	N	FLR	-	Head and neck	None
286011927	39	Un	D	F	Y	N	N	N	N	N	FC	-	Un	None
286028055	34	71	D	M	Y	N	N	N	N	N	FLR and/or FC	-	Un	None
339050695	31	44	D	M	Y	N	Y	N	N	Y	FLR	-	Head and neck	None
385147523	38	29	D	F	Y	N	Y	N	N	N	FLR	-	Un	None
537107148	56	36	D	F	Y	N	N	N	N	Y	Un	-	Dome and neck	None
551111590	30	56	P	M	Y	N	Y	N	N	N	FLR	-	Posterior process	TP
558022443	32	46	D	M	Y	N	Y	N	N	Y	FC	-	Neck	TP
608081447	33	63	D	M	Y	N	N	N	N	N	FLR	-	Lateral process	None
842004569	36	Un	D	F	Y	N	Y	N	N	N	FLR	-	Head	TP
852186228	36	Un	D	F	Y	N	N	N	N	N	FLR	-	Neck	TP & IP
397091820	38	41	D	F	N	Y	N	N	N	Y	-	-	-	None
852181163	34	Un	D	F	N	Y	N	N	N	N	-	-	-	TP & IP
116194	38	37	D	F	N	Y	N	N	N	N	-	-	-	None
122102	30	93	D	M	N	Y	N	N	N	Y	-	-	-	TP

397091820	38	41	D	F	N	Y	N	N	N	Y	-	-	-	None
100097193	37	Un	D	F	Y	N	N	N	Y	N	FLR	IP	Un	IP
608036775	43	35	D	F	N	N	N	N	Y	N	-	IP	-	None
116427	30	53	D	M	N	N	N	Y	N	Y	-	IP	-	None
852115721	45	50	P	F	N	N	N	Y	N	N	-	IP	-	None
852117115	52	87	D	M	N	N	N	Y	N	N	-	IP	-	IP
852139160	33	Un	D	M	N	N	N	Y	N	N	-	IP	-	TP

§ P: Passenger; D: driver
# M: Male; F: female
‡ Un: Unknown or not reported
ˆ FLR: Floor (including toe pan); FC: Foot controls (including parking brake)
° TP: Toe pan; IP: Instrument panel; None: No toe pan or instrument panel reported
*853200.2: talus fracture; 853414.2: medial malleolus; open/ displaced/ comminuted; 852200.2: metatarsal or tarsal fracture; 852400.2: patella fracture; 850826.2: knee sprain (not further specified); 851606.2: fibula fracture to head, neck, or shaft.

Conclusions

- The risk of injury to different body regions and the most frequent injuries of occupants with obesity are different than those of other occupants. This can be attributed to differences when interacting with the seat belt and vehicle interior.
- A likely explanation is that the increased risk of injury observed for occupants with obesity arises from their increased risk of injury to extremities and spine. Their increased risk of injury to the extremities can be attributed to their large forward motion during the crash and delayed engagement of the lap belt with the bony structure of the pelvis. The former is due to increased body mass, which results in increased kinetic energy, while the latter can be attributed to thick adipose tissue. These factors also cause a decreased torso forward pitch which increases compression force to the spine and elevates the risk of spinal injuries.
- An appropriate objective function for restraint optimization for occupants with obesity should incorporate the risk of injury to the extremities and spine.
- The HBMs should be instrumented properly to determine the risk of injuries, which were frequently observed in the field data.

Page intentionally left blank.

Part 2: Human Body Model Evaluation and Simulation Set-Up

Paper 2, Joodaki, Gepner, Katagiri, & Kerrigan, 2021a) further details the goals, methods, results, and conclusions of the study.

Relevance and Goal

Since this study aimed to use an HBM to predict injury in simulations designed to optimize the restraint system for an occupant with obesity, it was necessary to identify an appropriate HBM to serve the goals of this study. Thus, the objectives of this part were as follows.

- To determine whether an available obese HBM can be a suitable tool for designing a restraint system optimized for an occupant with obese anthropometry in the driver seat. To achieve this, the response of the HBM was compared to PMHS test results from the literature.
- To prepare the frontal impact driver-seat simulation environment necessary for restraint design parametric simulations, which are discussed in Part 3.

Methods

Obese Human Body Model Evaluation

The first subpart of Part 2, Joodaki, Gepner, Katagiri, & Kerrigan, 2021a), discusses the performance evaluation of an obese HBM. A family of obese HBMs with various heights and BMIs were previously developed by morphing a detailed midsize male HBM of the GHBMC M50-O v4.4 to statistically represent obese body shapes (Hu et al., 2016) (Figure 1).

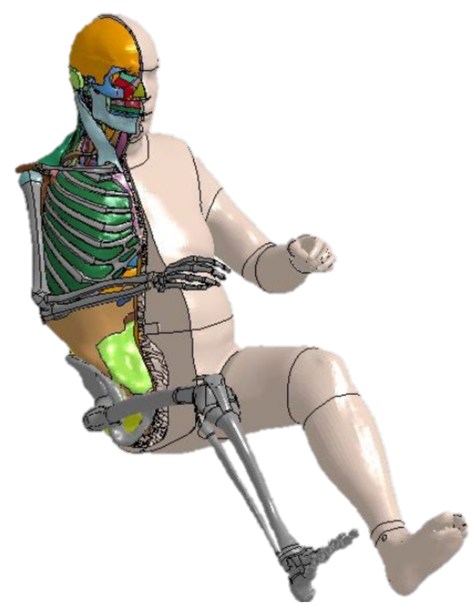

Figure 1. Obese HBM with BMI=35

Rear-seat tests: The results of 29 km/h and 48 km/h rear-seat sled tests with an obese PMHS (BMI=35 kg/m^2, stature=189 cm) were used to evaluate the performance of one of the obese HBMs (BMI=35 kg/m^2, stature=188 cm), replicating frontal sled test. To provide correct boundary conditions, a finite element model of the sled buck used in the PMHS tests were developed, validated, and used in the simulations (Figure 2-a).

Front-seat tests: The response of a midsize non-obese HBM (BMI=25 kg/m^2, stature=175 cm) and one of the obese HBMs (BMI=35 kg/m^2, stature=175 cm) were compared in a front-seat 56 km/h frontal impact test.

Model Set Up

The second subpart of Part 2 was to prepare the simulation environment for front-seat parametric simulations, which are discussed in Part 3. First, a simplified sled was generated from a Toyota Camry finite element model. The simplified model included seat structure, steering wheel, collapsible steering column, instrumentation panel, center console, floor, pedals, A-pillar, B-pillar, and driver-side door. A driver air bag (DAB) equipped with an adaptive vent and two types of knee air bags (KAB, low-mount and mid-mount) were added to the sled model. An obese HBM (stature = 175 cm, BMI 35 kg/m^2) and a midsize non-obese HBM (stature = 175 cm, BMI 25 kg/m^2) were positioned in the simplified sled (Table 7). Pre-simulations were performed to position them with similar head, torso, femur, and tibia angles. Virtual sensors were added to both HBMs to measure the risk of injury to different body regions. This included proper instrumentation for predicting the most frequent injuries, as identified in Part 1. Two types of seat belts, a regular seat belt and ISB, were routed on each HBM. Finally, an average pulse, which was determined from NHTSA's New Car Assessment Program (US-NCAP) 56 km/h frontal rigid-barrier tests with full-sized vehicles, was implemented into the sled (Figure 2-b).

(a)

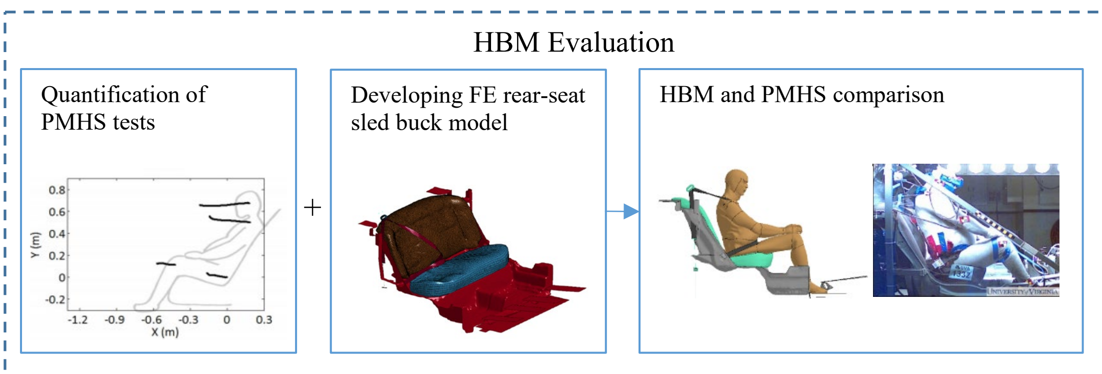

(b)

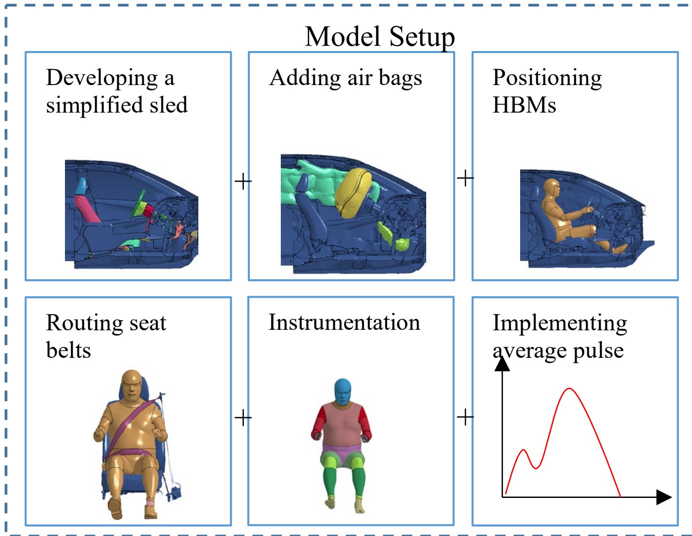

Figure 2. HBM evaluation (top) and model setup (bottom)

Table 7. Characteristics and positioning measurements of the subjects

	Obese HBM	**Non-Obese HBM**
Height (cm)	175	175
BMI (kg/m^2)	35	25
Age	30	30
Head Angle (deg)	78	79
Torso Angle (deg)	62	62
Femur Angle (deg)	17	17
Tibia Angle (deg)	48	48
H-Point Distance (cm)	9	8
Knee/Knee Bolster Distance (cm)	13	14

Head angle: the angle of line connecting the head CG to the shoulder with respect to a horizontal line.
Torso angle: The angle of line connecting the shoulder to the hip with respect to a horizontal line.
Femur angle: The angle of line connecting the hip to the knee with respect to a horizontal line.
Tibia angle: The angle of line connecting knee to the ankle with respect to a horizontal line.
H-point distance: the horizontal distance between the hip and the reference point on the back of the seat.
See Figure 3 for illustration of each parameter.

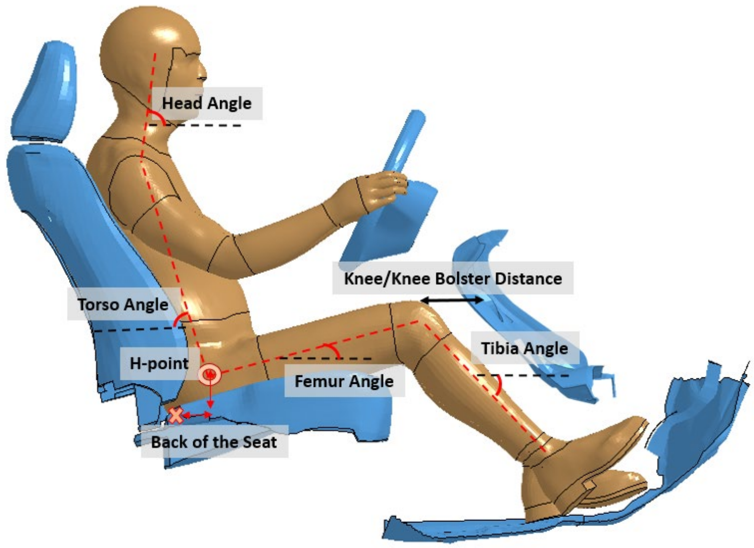

Figure 3. Description of positioning parameters of Table 7

Results

In the rear-seat tests both the obese HBM and the obese PMHS experienced a large forward excursion, delayed lap belt engagement with the pelvis, and maintained a reclined-to-upright torso angle throughout the tests (Figure 4). The PMHS demonstrated a submarining behavior in the 48 km/h test, starting when the hip traveled 18 cm, which was a consequence of the lap belt first loading the pelvis through the surrounding flesh and then sliding up over the pelvis into the abdomen as the pelvis translated downward compressing the seat. The HBM did not show a similar behavior, possibly due to a high stiffness of the flesh under shear loading (Figure 5).

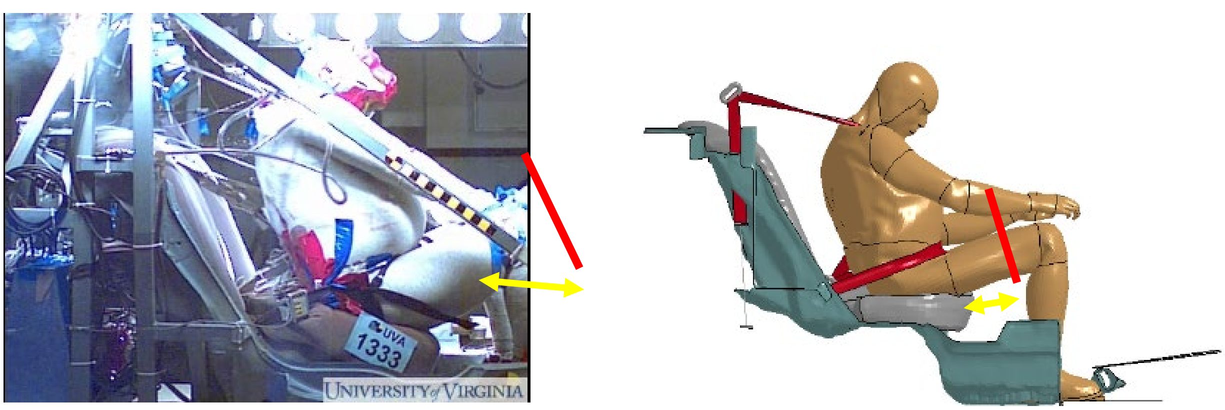

Figure 4. Comparison of behaviors of obese PMHS and obese HBM in 48 km/h rear-seat tests. Similarly, to obese PMHS, obese HBM experienced a large hip excursion and reclined torso throughout the test.

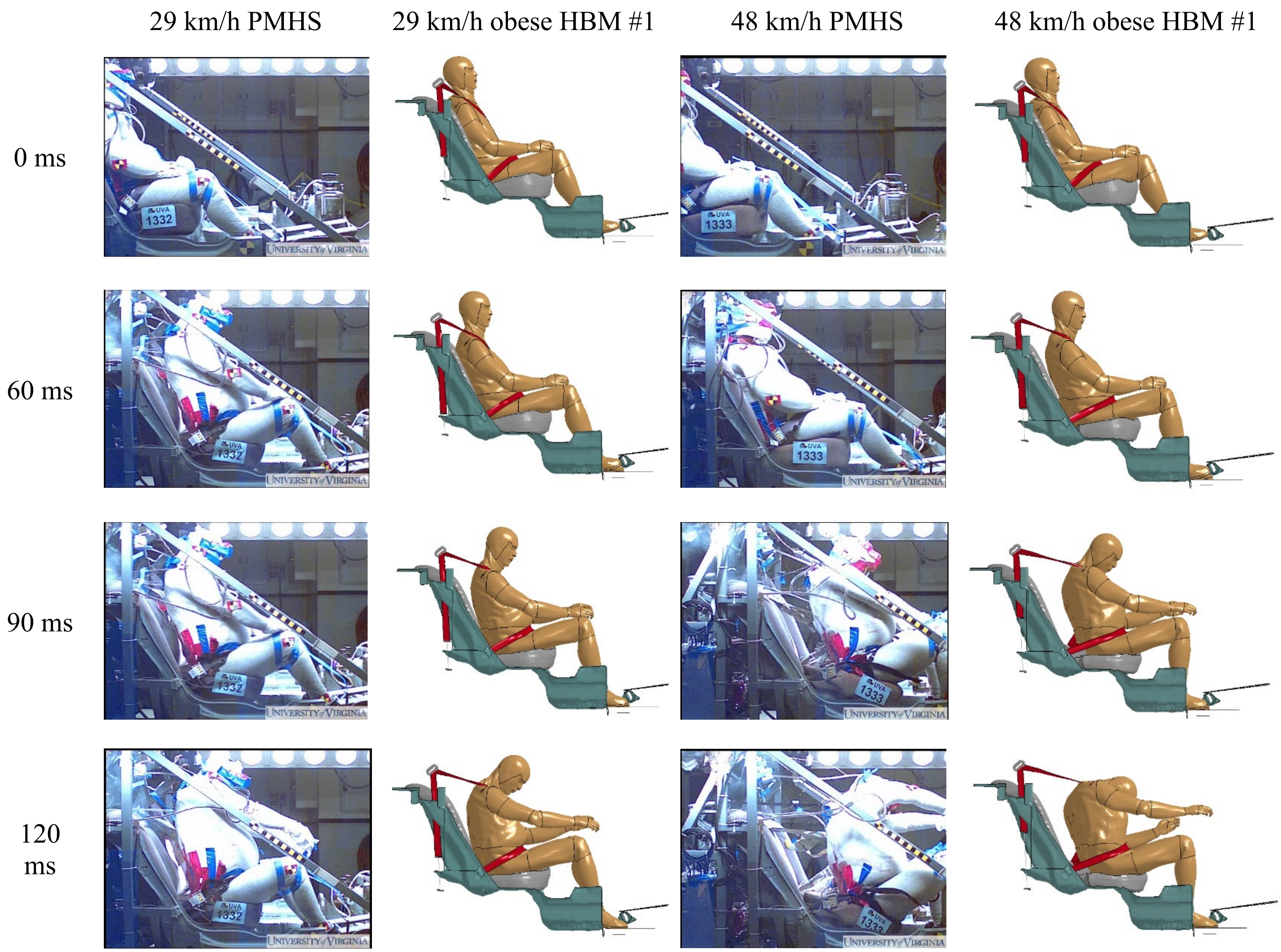

Figure 5. Comparison of behaviors of obese PMHS and obese HBM at 0, 60, 90, and 120 ms in rear seat tests

In the front-seat simulations (Figure 6), the obese HBM experienced a larger lower extremity excursion than the non-obese HBM. Furthermore, both obese and non-obese HBMs' pelvises traveled forward less than 12 cm because of the engagement between the knee and the knee air bag. This forward motion was shorter than the pelvis excursion of the PMHS (18 cm) when submarining was observed in the 48 km/h rear-seat test (Figure 7).

Non-Obese HBM front seat test | Obese HBM #2 front seat test

0 ms

60 ms

90 ms

120 ms

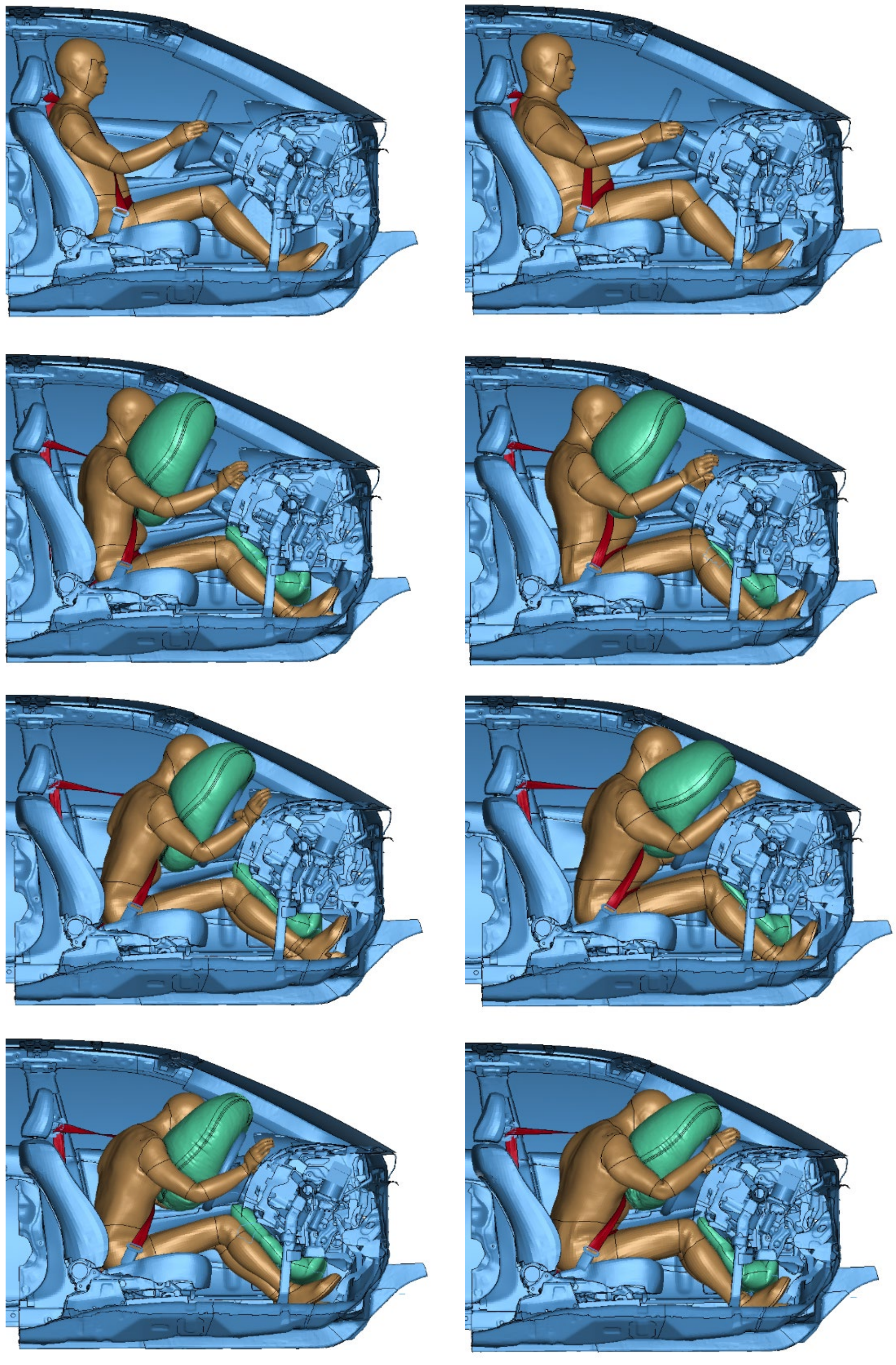

Figure 6. Comparison of response of non-obese HBM (left) and obese HBM #2 (right) at t=0 ms, t=60 ms, t=90 ms, and t=120 ms in 56 km/h frontal tests

(a)

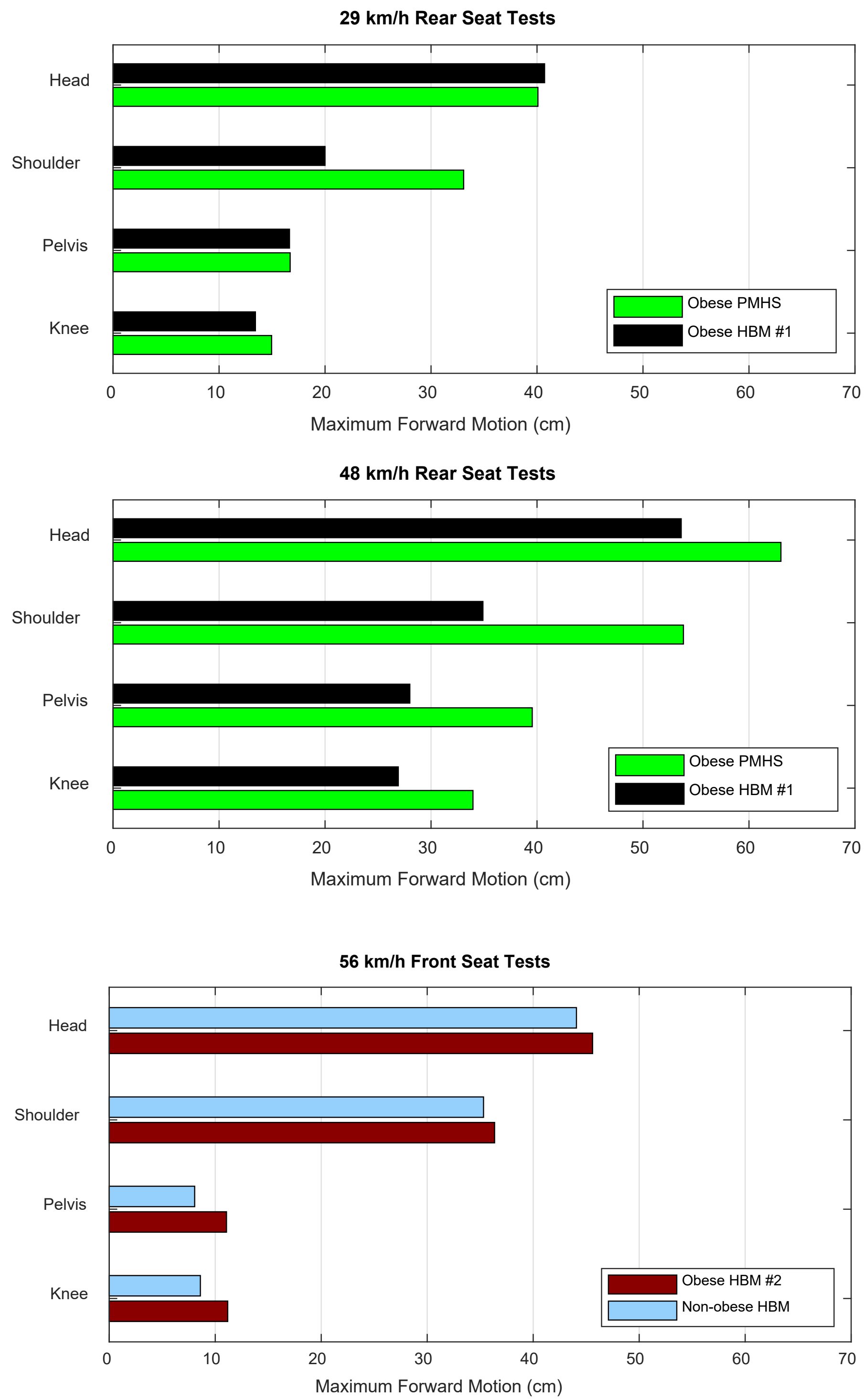

Figure 7. Maximum forward motion of different body segments during rear-seat (a) and front seat (b) tests

Conclusions

- The obese HBMs replicated the effects of large body mass and delayed lap belt engagement with the pelvis similarly to the obese PMHS. These characteristics are critical for front-seat frontal impact simulations.
- The obese HBMs failed to replicate submarining behavior observed in the high-speed rear-seat PMHS test. Nevertheless, since forward excursion of the front-seat occupants is limited by the vehicle structure or injury countermeasures, submarining is expected to be a less important issue when simulating crashes with the obese HBMs in the front-seat.
- Therefore, the obese HBMs can potentially still be useful tools for designing and optimizing restraint system for drivers with obesity.

Part 3: Parametric Simulations and Statistical Analysis

Paper 3, Joodaki, Gepner, & Kerrigan, J. (2020b) details the goals, methods, results, and conclusions of the study.

Relevance and Goal

Once the simulation environment had been constructed and the HBMs had been evaluated for suitability (Part 2), the next step was to begin simulating frontal crashes with the HBMs to identify trends and examine the effects of various restraint components that could be incorporated in the optimization part. Thus, the objective of this part was to perform parametric simulations to determine and compare the effect of different restraint parameters on the response of obese and non-obese HBMs through statistical and biomechanical analyses. These simulations were also used to train metamodels (Part 4), which were later used for restraint system optimization (Part 5).

Methods

Fourteen different restraint parameters along with the HBM type (obese versus non-obese) were selected as the simulation variables. Restraint parameters included: USAB presence and position; steering column failure level; presence of adaptive vent; DAB pressure; KAB pressure and type; presence of dynamic locking tongue (DLT); standard seat belt versus ISB; ISB pressure; shoulder belt load limiter type, constant versus digressive; load limiter force level (LL); presence anchor and buckle pre-tensioner. The lower-bound and upper-bound of each variable were specified. The Latin Hypercube technique was used to sample 450 simulations in this 15-dimensional design domain. Then, the parametric simulations were performed, and the results of the parametric simulations were extracted and used to determine excursion (kinematics) of, and risk of injury to, different body regions. Injury measures included: Head Injury Criterion (HIC) (Versace, 1971), Brain Injury Criterion (BrIC) (Takhounts et al., 2013), Neck Injury Criterion (NIC) (Eppinger et al., 2000), normalized chest compression (Cmax) (Kent & Patrie, 2005), peak lumbar force, peak femur force, peak patella force, and Revised Tibia Index (RTI) (Kuppa et al., 2001). This information along with the NASS-CDS field data (Part 1) were used to calculate life years lost (LYL) (Kim et al., 2019; Bollapragada, 2019). Multivariate regression analyses were performed to determine and compare the effects of different restraint parameters on the responses of obese and non-obese HBMs. Finally, the biomechanical reasons of the findings were discussed in detail (Figure 8).

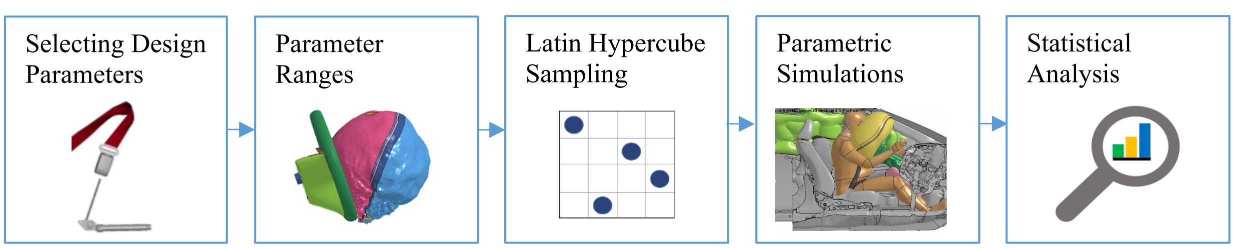

Figure 8. Flow chart of the Part 3

Results

The obese HBM experienced significantly greater lower extremity excursion, and injury metric values for chest, neck, lumbar spine, femur, patella, and tibia than the non-obese HBM (Figure 9). For both occupants, increasing the seat belt LL level resulted in increased head, neck, and chest injury metrics. Also, the ISB decreased the HBMs' excursion, and chest and neck injury metrics. The USAB and mid-mount KAB decreased lower extremity excursion, and the USAB mitigated the obese HBM's femur, patella, and tibia injury metrics. The USAB increased the non-obese HBM's neck and lumbar spine injury metrics (Figure 10 and Figure 11).

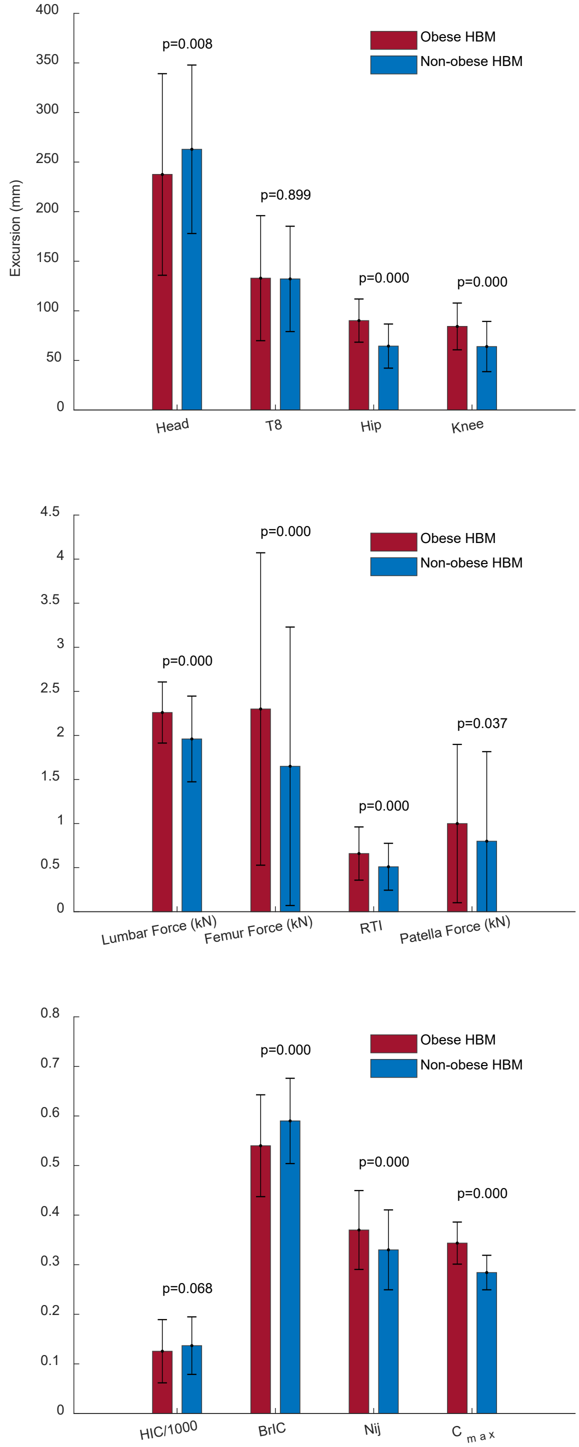

Figure 9. Comparison of responses of obese and non-obese HBMs in parametric simulations

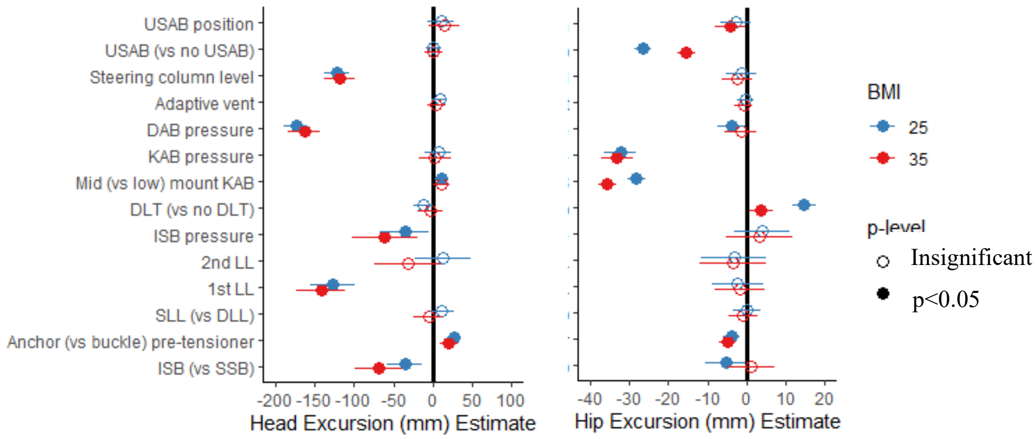

Figure 10. Effects of different restraint parameters on the head and hip excursion shown using forest plots of multivariate regression analyses on results of parametric simulations with obese (red) and non-obese (blue) HBMs. Solid circles show a statistically significant correlation between the simulation inputs (restraint parameters) and outputs (head and hip excursions)

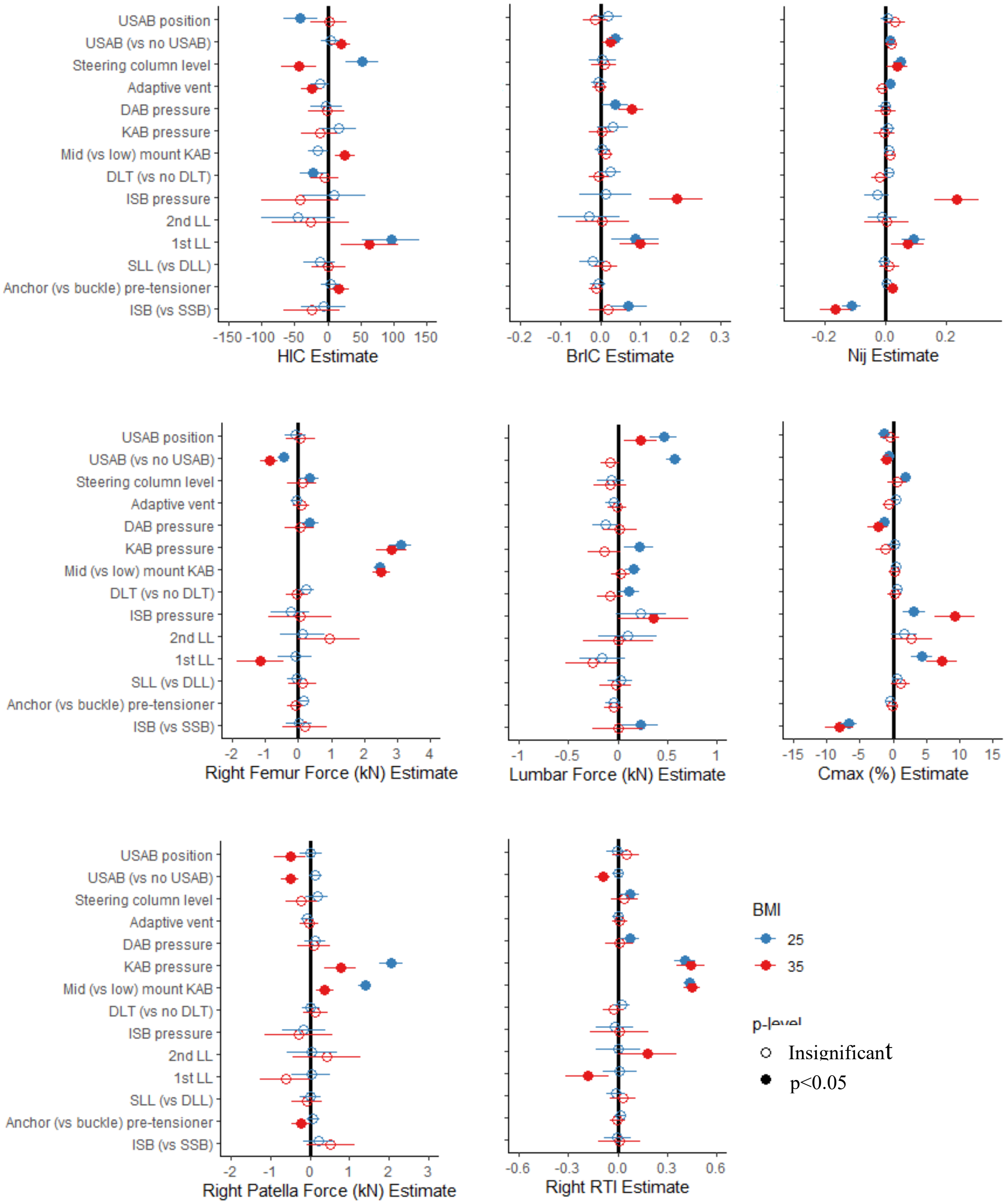

Figure 11. Forest plots of multivariate regression analyses on the effects of different restraint parameters on various injury metrics

Conclusions

- The replicated HBMs represented some key biomechanical differences between occupants with and without obesity.
- The general strategies typically used to improve safety of non-obese occupants were not found to have any compelling counter-effects for the occupant with obesity.
- However, the effect of obesity, which was included as a difference in the HBMs, resulted in a difference in the value of injury metrics across a range of parameters.
- The findings suggested that solutions should be focused on arresting lower extremity excursion to decrease lower extremity injuries for the obese HBM. This confirmed the hypothesis in Part 1: the key for increasing the safety of occupants with obesity is to mitigate their lower extremity excursion. For example, the USAB was found to reduce both the lower extremity excursion and injury metric values and thus might be a useful tool to improve the safety of occupants with obesity. Also, the ISB was found to be an effective countermeasure to decrease the occupant's chest and neck injuries.
- For several restraint parameters, manipulation was found to decrease the risk of injury to a body region but increase the risk to another region. Hence, a comprehensive restraint system optimization with a range of anthropometries is necessary to find the most favorable set of restraint parameters.

Part 4: Metamodel Development

Paper 4, Joodaki, Gepner, & Kerrigan (2020b), details the goals, methods, results, and conclusions of the study.

Relevance and Goal

Next, we used the simulation results from Part 3 to mathematically model the relationships between the simulation inputs and outputs. The mathematical models (metamodels) were intended to mimic the behavior of the system (simulation results) in a continuous space, which would permit exploring the whole design domain (Part 5) with a more manageable computational cost than the traditional optimization approach (iterative process of guessing a solution and running simulation with the guessed solution). Thus, the objectives of this part were to:

1) Develop metamodels of the parametric simulation results (from Part 3), which were later used for restraint system optimization (Part 5).
2) Demonstrate in detail how machine learning can be leveraged for predicting HBM responses to avoid model over-fitting and under-fitting (Figure 12).
3) Compare the ability of OLS, least absolute shrinkage, and selection operator (LASSO), neural network (NN), support vector regression (SVR), regression forest (RF), and an ensemble model for predicting the results of restraint design parametric simulations.

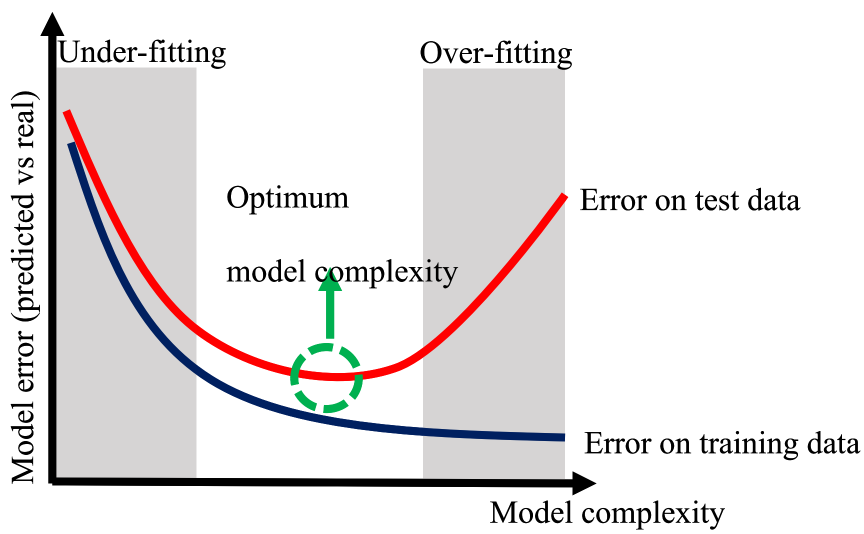

Figure 12. Illustration of over-fitting and under-fitting

Methods

Metamodels for LYL (optimization objective function for Part 5), chest deflection, and head-steering column distance (optimization constraints for Part 5) were developed through a similar process. For each of those dependent variables, the hyperparameters (parameters whose values should be set by user before training) of LASSO, NN, RF, and SVR were optimized using grid search and 10-fold cross-validation to avoid over-fitting and under-fitting. A linear OLS fit and an ensemble model, which combined the optimized LASSO, NN, RF, and SVR models, were also developed. The accuracy of the models, which were developed using different techniques, were compared through leave-one-out cross-validation and the model with the highest accuracy was selected to be used for restraint system optimization (Part 5, Figure 13).

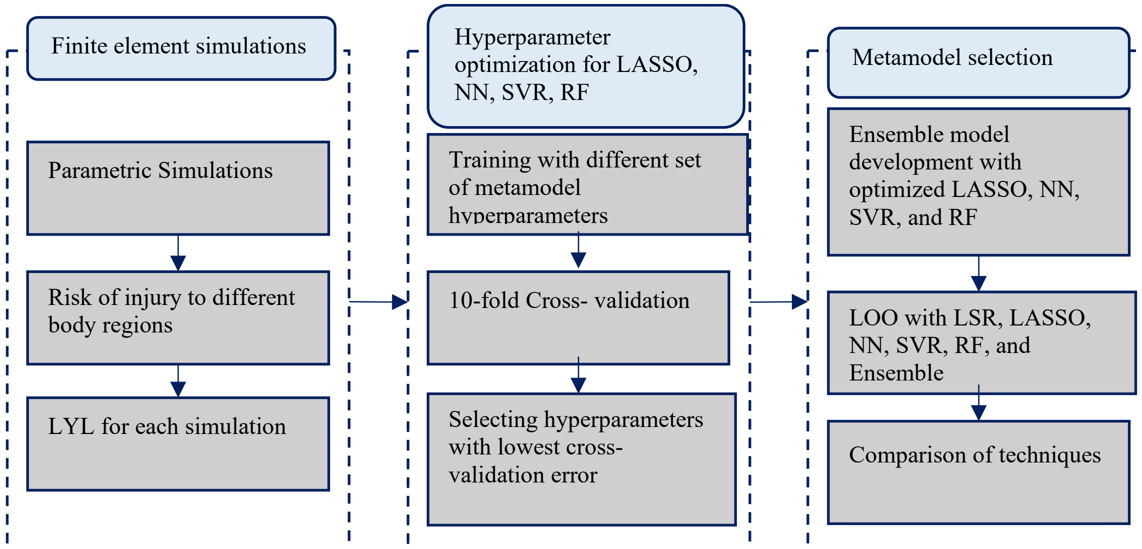

Figure 13. Procedural flowchart for metamodel development

Results

- When the hyperparameters were optimized, the prediction error decreased by up to three times compared to some models with random (not optimized) hyperparameters, which were developed with the same regression technique.
- Different machine learning models, which were developed using distinct and different algorithms, predicted a similar LYL contour when their hyperparameters were optimized (Figure 14).
- The shapes of the response surfaces predicted by the metamodels were shown to be dependent on the values of hyperparameters (Figure 15).
- The ensemble method outperformed all other techniques regardless of the dependent variable for which the metamodel was developed (LYL, chest deflection, head-steering column distance, Figure 16).

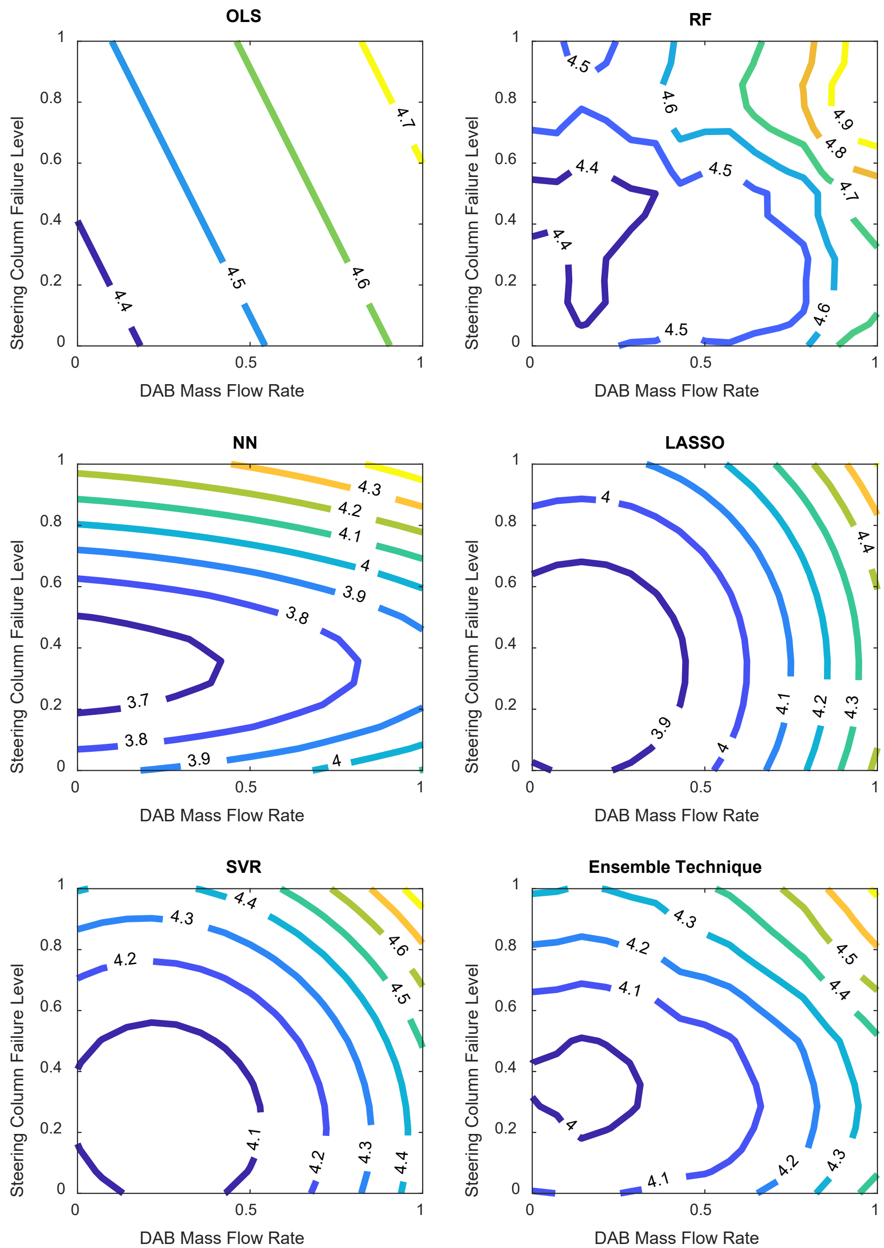

Figure 14. An example of LYL prediction contours with different normalized DAB mass flow rate and steering column failure level values using different techniques with optimized hyperparameters. Other simulation parameters were constant in these predictions: obese occupant, regular seat belt with a digressive LL (2 kN and then 1 kN) and anchor pre-tensioner, dynamic locking tongue, adaptive vent, 65 kPa low-mount KAB, and no USAB.

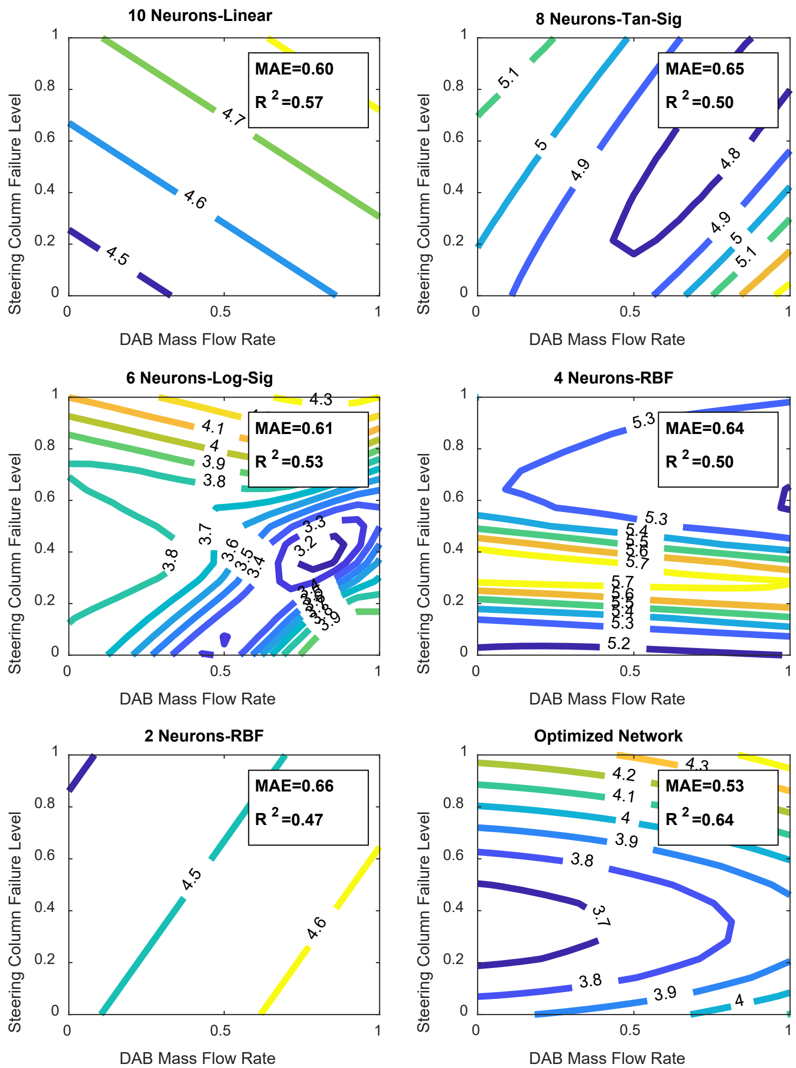

Figure 15. Comparison of LYL contours predicted by networks from different transfer functions and number of neurons developed using unoptimized and optimized (number of neurons: 4, transfer function: Tan-Sig) hyperparameters. The leave-one-out cross-validation errors of each model are also shown. Other simulation parameters were the same as in Figure 8.

(a)

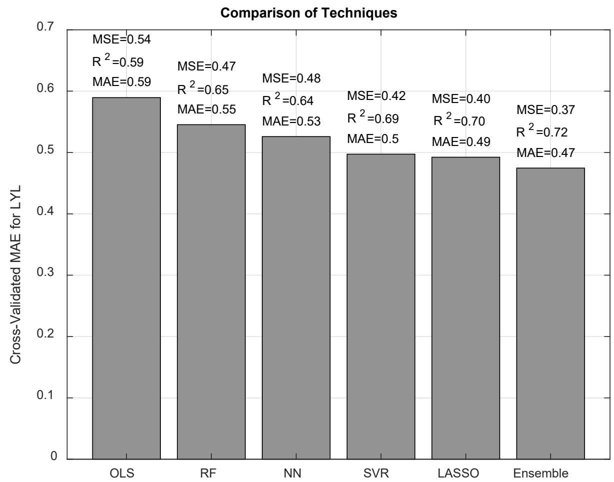

(b)

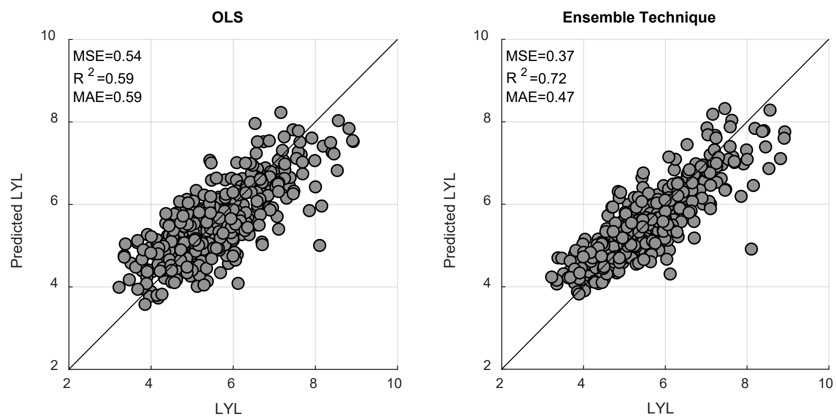

Figure 16. (a) Comparison of leave-one-out cross-validation mean absolute error (MAE) for life years lost (LYL) metamodels developed using OLS, RF, NN, LASSO, SVR and ensemble model. The hyperparameters of RF, NN, LASSO, SVR, and ensemble techniques were optimized prior to leave-one-out cross-validation. Mean squared error (MSE) and coefficient of determination (R^2) are also shown (b) leave-one-out cross-validation scatter plots of OLS (left) and ensemble technique (right).

Conclusions

- Machine-learning techniques showed a higher prediction accuracy compared to linear OLS. In addition, if linear OLS is used for the optimization, the optimization process would converge to the boundary of the design space. Hence, machine learning techniques used in this part are more suitable than the linear OLS for developing metamodels, which would be used for restraint system optimization.
- The goal here was to create metamodels that would be subjected to an optimization algorithm in the next part. Therefore, the metamodels should be able to capture the correlation pattern between the design parameters and the objective function. As the shape of the response surface approximated by the metamodels is dependent on the value of their hyperparameters, optimizing hyperparameters is crucial for the metamodels that are developed for restraint system optimization. Solely selecting some hyperparameters

without optimization and then training the metamodel might result in failing to find the actual optimized design.

- Some commercial optimization software packages offer optimization approaches that involve training metamodels, but they do not offer the option to tune hyperparameters prior to training the models automatically. Data from this study suggests that tuning the hyperparameters prior to training the models results in better cross-validation errors across all methods.

Part 5: Restraint System Optimization

Gepner, Lee, Katagiri, Kim, & Kerrigan (2021b), details the goals, methods, results, and conclusions of the study.

Relevance and Goal

In Part 4 tuned metamodels were developed for the LYL (the optimization objective function, see Part 5 methods), chest deflection (an optimization constraint, see Part 5 methods), and head-steering column displacement (an optimization constraint, see Part 5 methods) using the ensemble method. Next, it was aimed to use those metamodels to perform restraint system optimization. Thus, the objective of this part was to optimize the restraint system for the following.

1) HBM with obese anthropometry (BMI=35)
2) HBM with non-obese anthropometry (BMI=25)
3) Obese (BMI=35) and non-obese (BMI=25) HBMs concurrently

The research question was whether an optimized restraint system for an occupant with obesity would be different than that for a midsize occupant.

Methods

As mentioned in Part 3, virtual sensors were mounted on different body regions of the HBMs. Since (1) an effective restraint system should protect the occupant against fatal injuries and (2) seven out of 10 most common injuries of obese occupants were found to be non-fatal lower extremity injuries (Part (1), which could affect the occupant's life quality, both fatal and non-fatal injuries had to be considered for optimization. The risks of injuries to different body regions had to be combined into a single metric to be used as the objective function. LYL, which is a metric that incorporates the risk of fatal and non-fatal injuries to different body regions (Table 8), was considered as the optimization objective function for the first two optimization cases (optimization for the obese and non-obese HBMs independently). The details of how this metric is calculated from simulation results are provided in Kim et al. (2019) and Bollapragada (2019). The objective function in the third case (concurrent optimization) weighted LYL between both occupants equally, but also included a difference term to avoid a solution which is substantially

$$\begin{cases} \min[LYL(\boldsymbol{X})] \\ subject\ to: \\ HIC, Nij, NeckT\ or\ NeckC, ChestC, FemurF < 80\ \% \times NHTSA\ IARVs \\ Head\ to\ steering\ wheel\ distance > 40\ mm \\ \boldsymbol{X}_{\boldsymbol{lower\ bound}} \leq \boldsymbol{X} \leq \boldsymbol{X}_{\boldsymbol{upper\ bound}} \end{cases}$$

in favor of a single HBM: $\min[LYL_{obese} + LYL_{non-obese} + |LYL_{obese} - LYL_{non-obese}|]$. The NHTSA injury assessment reference values, as well as head-steering column distance, were considered as the optimization constraints.

A genetic algorithm was applied to the metamodels of the objective function and constraints (developed in Part 4) to find the optimal design. The functions used for the fitness scaling, selection, initial population creation, crossover, and mutation of this genetic algorithm were rank-based, stochastic uniform, uniform, scattered, and Gaussian, respectively (see for details about each of these functions). An improvement-based stop criterion was used for the genetic algorithm. Once the genetic algorithm stopped iterating, a finite element simulation with the selected design was run. Then, LYL was calculated using the finite element simulation results and compared to the LYL value previously predicted by the LYL metamodel. If the difference between the two values was less than 0.1, the optimization solution was accepted. Otherwise, the results of the new finite element simulation were added to the point cloud, the metamodels were updated, and the optimization process was repeated (Figure 17).

To understand the contribution of different injury metrics or body regions to the LYL value, the following analysis was performed for each injury metric/body region.

1. LYL value was calculated for each test of the initial 450 parametric simulations.
2. For each injury metric/body region, the associated AIS2+ injury risks were reduced to zero in each simulation.
3. A new LYL value was calculated with injury risks from step 2 for each simulation.
4. The LYL value from step 3 was compared to the original LYL value from step 1 for each simulation. The magnitude of difference between step 3 LYL and step 1 LYL was the contribution of that injury metric/body region to the LYL value.
5. Mean and standard deviations of contributions in the initial 450 parametric simulations were determined.

Table 8. List of HBM instrumentations and injury metrics used for LYL calculation

Body Region	Location	Instrumentation	Metric	Reference
Head	Skull and brain	Head CG Node output	HIC	Versace, 1971
	Brain	Head CG Node output	BrIC	Takhounts et al., 2013
Face	Frontal bone (LR)	Contact force output	Force	Cormier et al., 2011a
	Maxillar bone (LR)	Contact force output	Force	Cormier et al., 2011b
	Nasal bone	Contact force output	Force	Cormier et al., 2010
Neck		Cross section output	NIJ	Eppinger et al., 2000
Thorax		Sternum and vertebra node output at different levels	Cmax	Kent & Patrie, 2005
		Rib cage nodes output	Deflection at several locations (Rmax)	NHTSA, 2015
Abdomen		Abdomen flesh and vertebra node output	Cmax	Kent et al., 2008
Lumbar spine		Lumbar spine beams output	Axial force	Stemper et al., 2015
Upper extremity	Clavicle (LR)	Cross section output	Bending moment	Zhang et al., 2013
	Humerus (LR)	Cross section output	Bending moment	Santago et al., 2008
	Forearm (LR)	Cross section output	Bending moment	Duma et al., 2002
	Wrist (LR)	Cross section output	Axial force	Duma et al., 2003
Lower extremity	Hip (LR)	Contact force output	Axial knee force	Rupp et al., 2010
	Femoral neck (LR)	Cross section output	Force	Roberts et al., 2010
	Knee-thigh-hip (LR)	Cross section output	Femur axial force	Kuppa et al., 2001)
	Femoral shaft (LR)	Cross section output	Moment	Kerrigan et al., 2004
	Femoral condyle (LR)	Cross section output	Moment	Rupp et al., 2010

Cont.	Patella (LR)	Cross section output	Force	Kuppa et al., 2001
	Revised Tibia Index	Cross section output	Force and moment	Kuppa et al., 2001
	Tibia plateau (LR)	Cross section output	Axial force	Hirsch & Sullivan, 1965
	Tibia shaft (LR)	Cross section output	Moment	Kerrigan et al., 2004
	Distal tibia (LR)	Cross section output	Force	Kuppa et al., 2001
	Tibia shaft (LR)	Cross section output	Revised Tibia Index	Kuppa et al., 2001
	Ankle (LR)	Cross section and beam output	Tibia an Achilles force	Funk, Crandall, et al., 2002a
	Foot/Ankle (LR)	Node and cross section output	In/eversion angle and tibia axial force	Funk, Srinivasan, et al., 2002b
	Foot/Ankle (LR)	Node, beam, and cross section output	Dorsiflexion and tibia force	Funk, Srinivasan, et al., 2002b

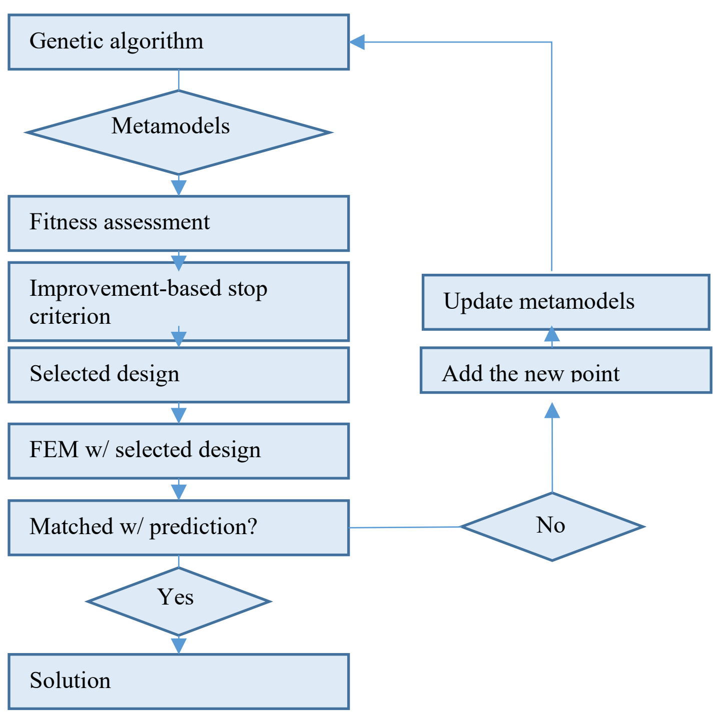

Figure 17. Flow chart of restraint system optimization

Results

In general, while the restraint parameters were similarly distributed between the obese and non-obese HBM simulations, the obese HBM experienced a higher LYL value than the non-obese HBM (Figure 18). The LYL values with the optimized design for obese and non-obese HBMs were lower than the LYL value in any parametric simulation. In other words, the optimization process identified a combination of restraints that was not tried in the parametric simulations and yet, it was more advantageous than any of the combinations, which were tried in the parametric simulations. That suggests that the LYL metamodel developed in this study (Part 4) successfully modeled the response surface of the system and the genetic algorithm found the optimum of that surface. In addition, the injury risks to different body regions were lower with the optimized designs than the average of those injury risks in parametric simulations.

Analysis on the parametric simulations showed that the risk of injury to brain had the highest contribution to the LYL among different body regions. For the obese HBM and non-obese HBMs, the risks of injury to the lower extremity and spine were the second main contributors to the LYL, respectively (Figure 19).

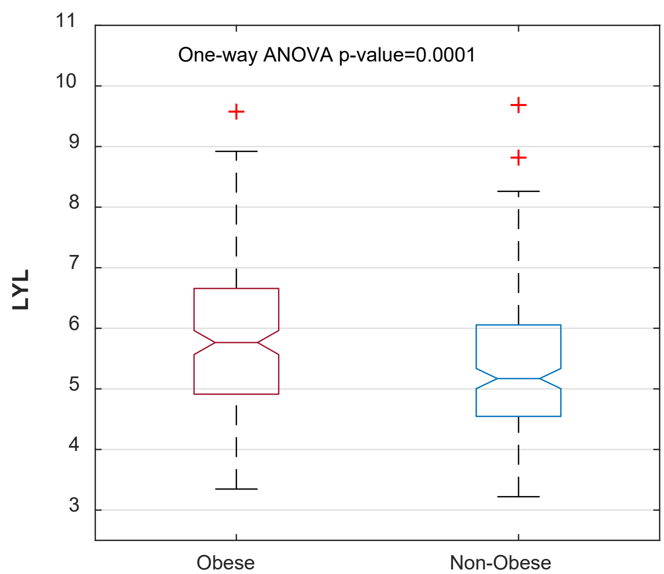

Figure 18. Box plot of LYL values in the initial 450 parametric simulations. Obese HBM experienced a significantly higher LYL value than non-obese HBM

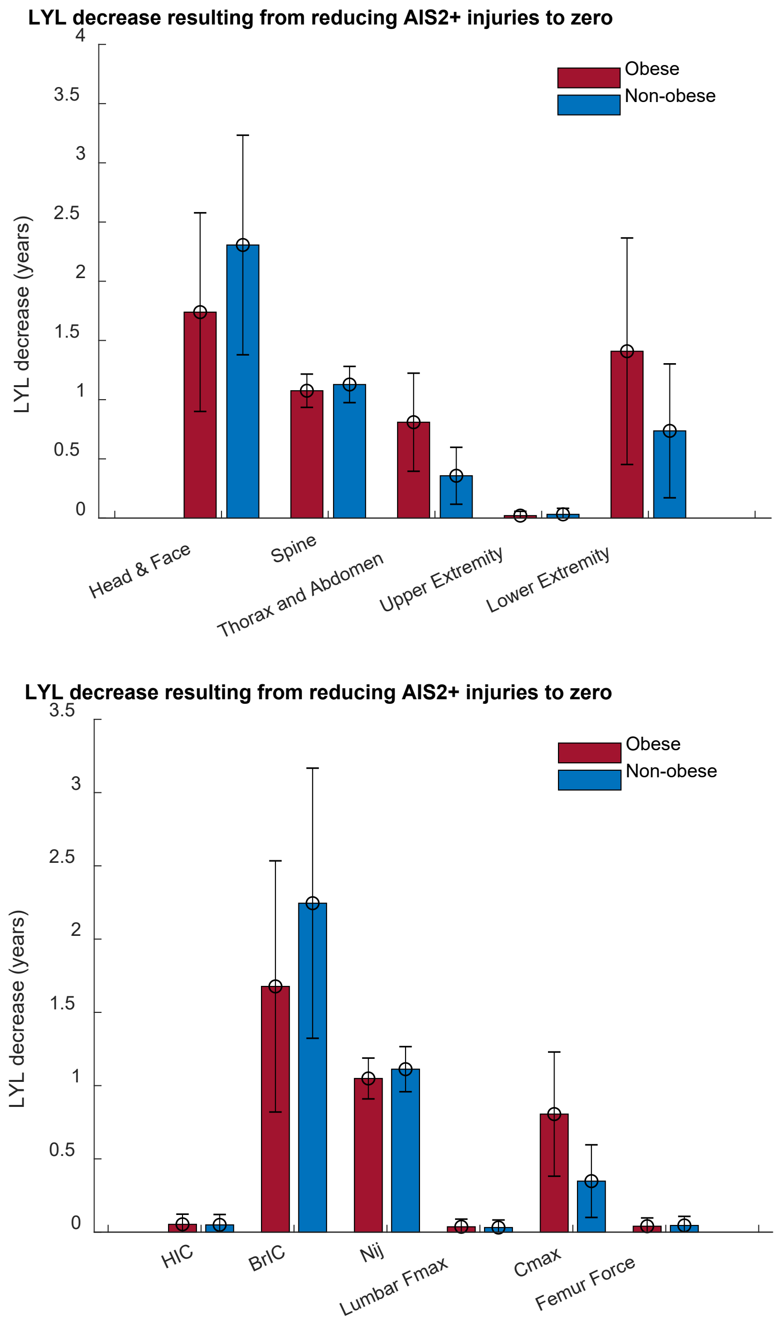

Figure 19. Contribution of different body regions (top) and some injury metrics (bottom) to LYL value in the initial 450 parametric simulations. The contribution values are determined by comparing the original LYL values to new LYL values after reducing associated AIS2+ injuries to zero for each simulation.

Optimum Design for Obese Versus Non-Obese HBMs

The optimized value of some parameters was identical between the obese and non-obese HBMs. For both HBMs, a 65 kPa inflatable (versus regular) seat belt with anchor-side (versus buckle-side) pre-tensioner was found to be optimal. Also, the optimal restraint system for both occupants included a 47 kPa DAB with an adaptive vent and a 50 kPa mid-mount KAB.

However, there were some differences in the optimized design parameters between the two HBMs. The optimum LLs for the obese and non-obese HBMs were constant (1.5 kN) and digressive (1.5 kN followed by 1 kN), respectively. Additionally, the optimum steering column failure levels for the obese and non-obese HBMs were 4.6 kN and 5.4 kN, respectively. Also, the optimized restraint for the obese HBM included the USAB positioned close to the front edge of the seat, while the non-obese optimum design did not have the USAB (Figure 20 and Table 9).

The design sensitivity analysis, which was performed using metamodels, revealed that changing the seat belt type, first LL level, existence of USAB and its position, and DAB pressure had the greatest effects on the LYL value (Figure 21).

The optimal value of some design parameters, including inflatable belt and KAB pressures, were at the lower bound. The lower-bound pressure was the minimum pressure with which, the air bag model could correctly deploy. To make sure that convergence of KAB pressure at the lower-bound does not imply that not using a KAB is more beneficial than using it, two simulations with the optimized designs for obese and non-obese, but with no KAB, were performed. The results showed that not using a KAB was associated with increasing LYL value from 2.90 to 3.32 for the obese HBM and 2.99 to 3.11 for the non-obese HBM. Hence, using a low-pressure KAB was beneficial for protecting the occupants. Also, using a low-pressure (versus high-pressure) inflatable belt was beneficial as it could flatten on the chest and distribute the force to a wide area (Figure 22).

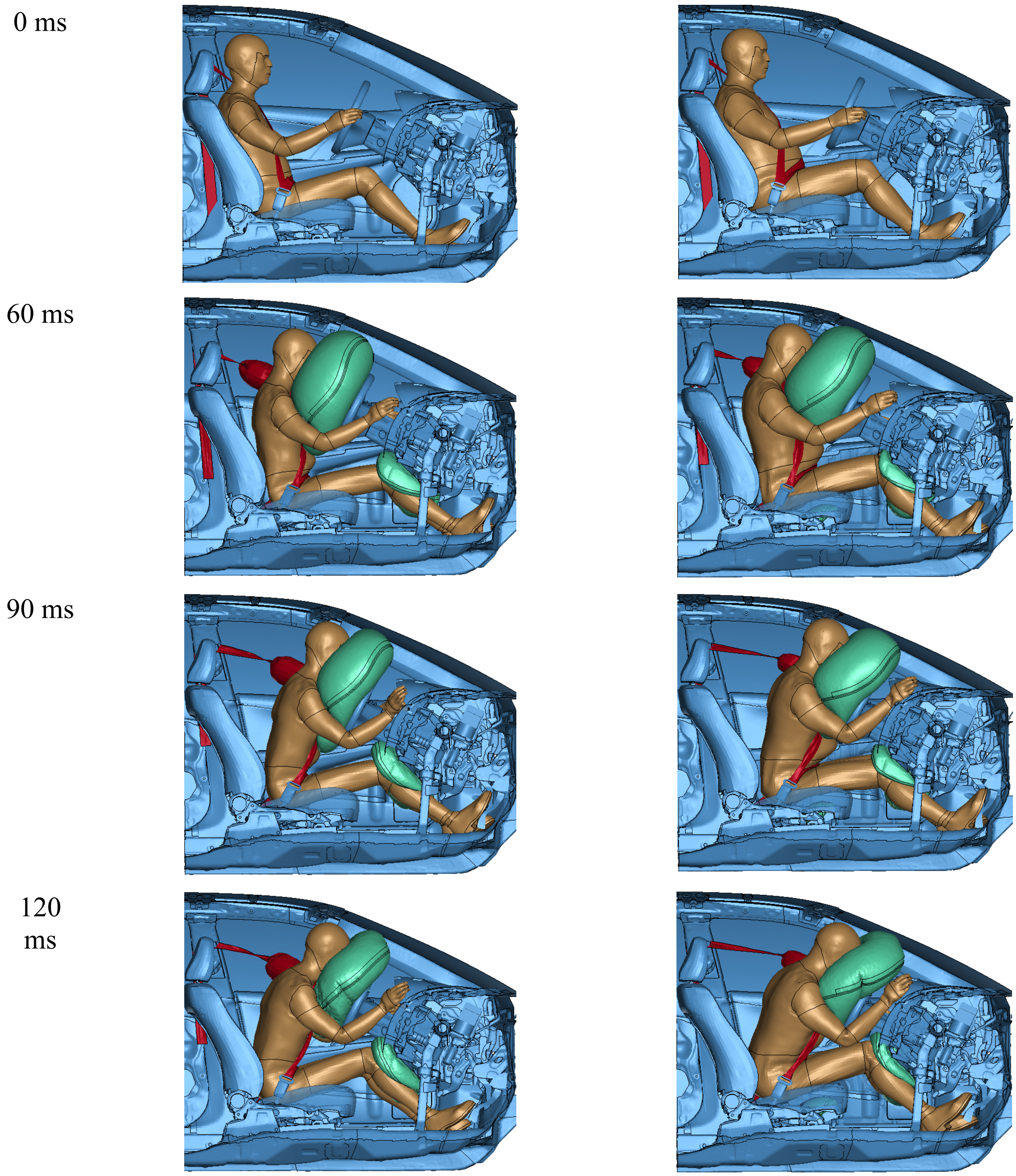

Figure 20. The response of non-obese (left) and obese (right) HBMs in frontal impact simulations with their optimized designs

Table 9. Optimization parameters, their lower and upper bounds, and their optimized value for obese HBM, non-obese HBM, and concurrent optimizations

	Parameter	Range	Baseline design	Optimized for obese	Optimized for non-obese	Optimized concurrently
1	Air-belt (vs regular belt)	binary	Regular belt	Air-belt	Air-belt	Air-belt
2	Air-belt pressure (kPa)	65–300	-	65	65	65
3	Anchor (vs buckle) pre-tensioner	binary	Anchor	Anchor	Anchor	Anchor
4	Level of first LL (kN)	1.5–9	3	1.5	1.5	1.5
5	Switchable (vs constant) LL	binary	Constant	Constant	Switchable	Constant
6	Level of second LL (kN)	1–6	-	-	1	-
7	DLT (vs regular tongue)	binary	Regular tongue	DLT	DLT	DLT
8	Active vent	binary	Not adaptive	adaptive	adaptive	adaptive
9	Driver air bag pressure (kPa)	3–150	24	47	47	47
10	Mid-mount (vs Low-mount) KAB	binary	Low-mount	Mid-mount	Mid-mount	Mid-mount
11	KAB pressure (kPa)	50-300	133	50	50	50
12	USAB (vs no USAB)	binary	No USAB	USAB	No USAB	No USAB
13	USAB Position (mm)	-138–0	-	0	-	-
14	Collapsible steering column failure level (kN)	1.5–6.3	3	4.6	5.4	4.9
	LYL value	$Obese_{avg}$:5.82* Non-$Obese_{avg}$:5.36*	Obese: 3.31 Non-Obese: 3.31	Obese: 2.90	Non-Obese: 2.99	Obese: 3.19 Non-Obese: 3.07

*: Mean values from parametric simulations

USAB Position: Fore-aft position of USAB with respect to the front edge of the seat

The air bag pressure lower bounds were the minimum pressure, at which, the air bag model could fully deploy. To reach the desired pressures, mass flow rates were scaled.

All reported pressures are relative to the atmospheric pressure (101 kPa) and from air bag deployment static tests with optimized mass flow rate scale factor.

A DLT was used in all simulations with the inflatable seat belt.

Reported LYL values are for 56 km/h tests.

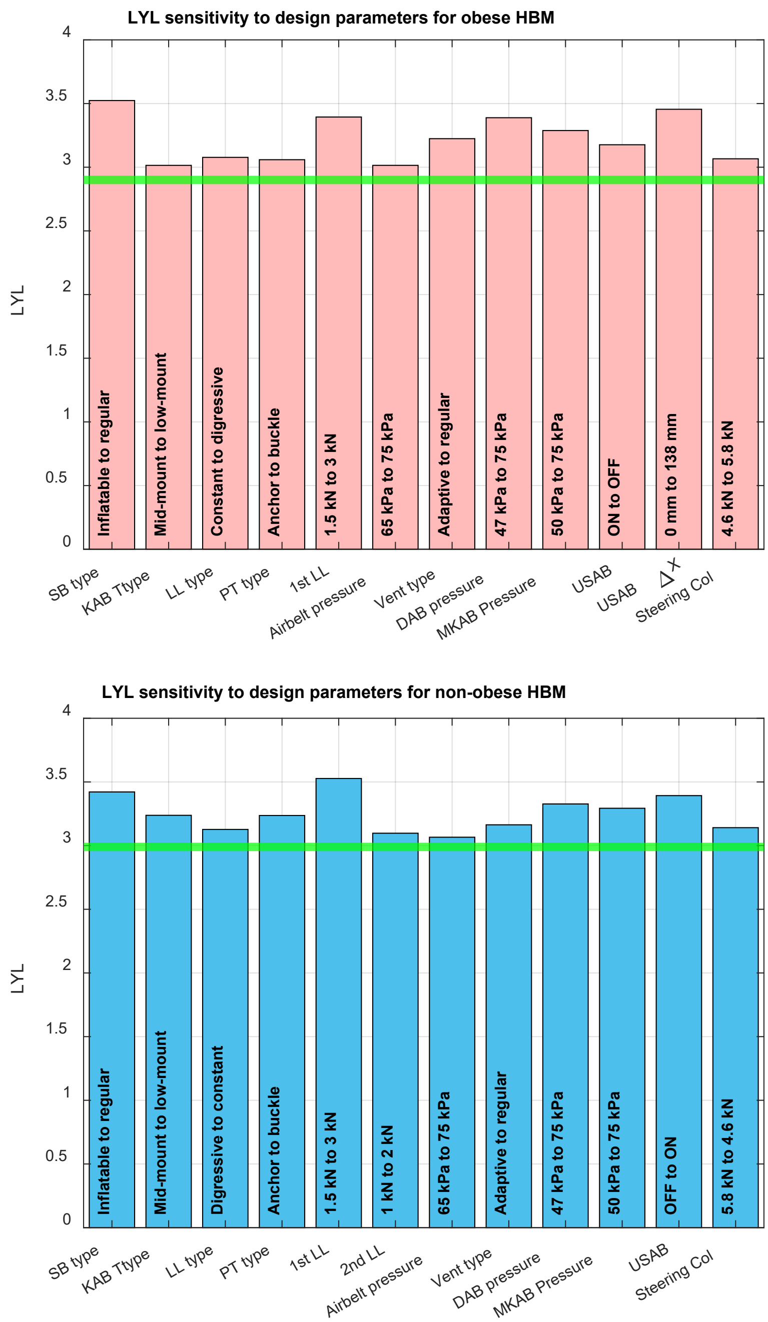

Figure 21. Sensitivity of LYL to design parameters of optimized restraint system for obese (top) and non-obese (bottom) HBMs, determined from LYL metamodel. The green horizontal line shows LYL value with optimized design.

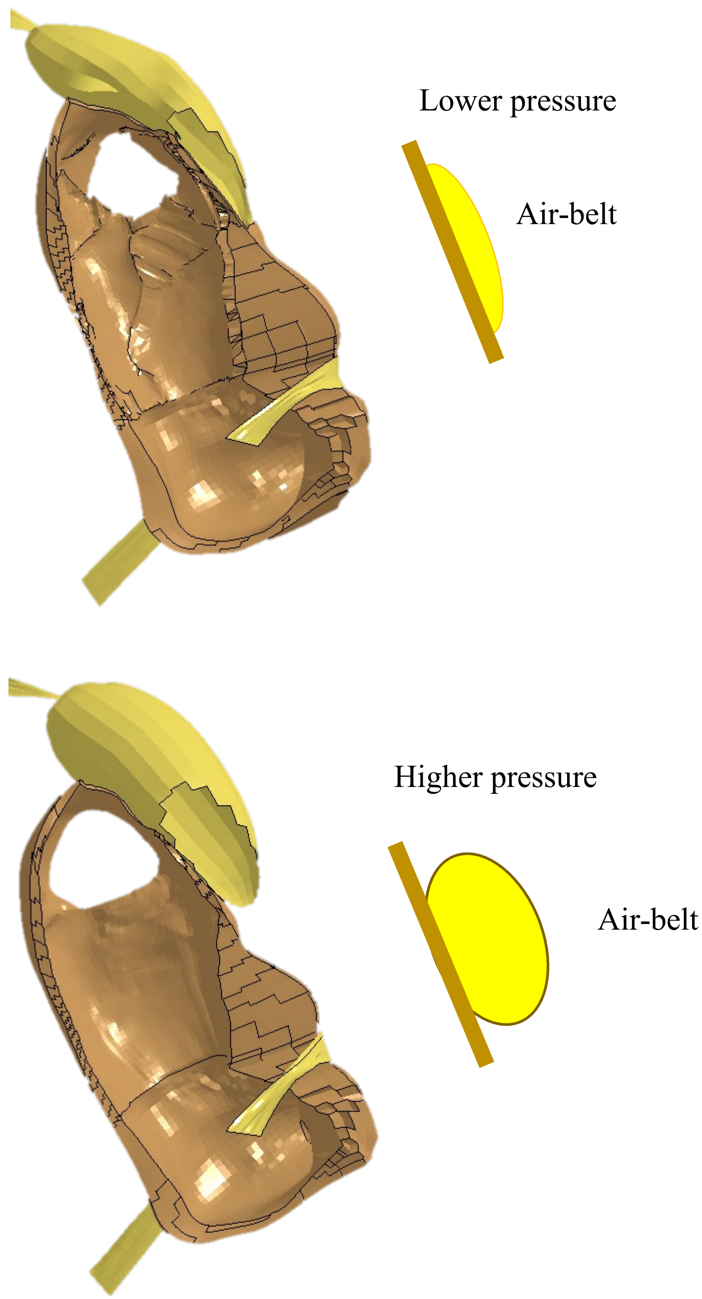

Figure 22. With a low-pressure air-belt, the ISB could flatten on the chest and more effectively distribute seat belt force and mitigate localized chest deformations.

Concurrent Optimization for Obese and Non-Obese HBMs

The restraint system, which was optimized for obese and non-obese HBMs concurrently, included a 65 kPa ISB with 1.5 kN constant LL, anchor pre-tensioner, 47 kPa adaptive vent DAB, 50 kPa mid-mount KAB, and 4.9 kN collapsible steering column. This restraint system did not include the USAB (Table 9). The LYL value for the obese HBM with this design was higher compared to the non-obese HBM. Further, the LYL values for the obese HBM and the non-obese HBM were higher than they were for the restraint systems optimized for each of the occupants separately.

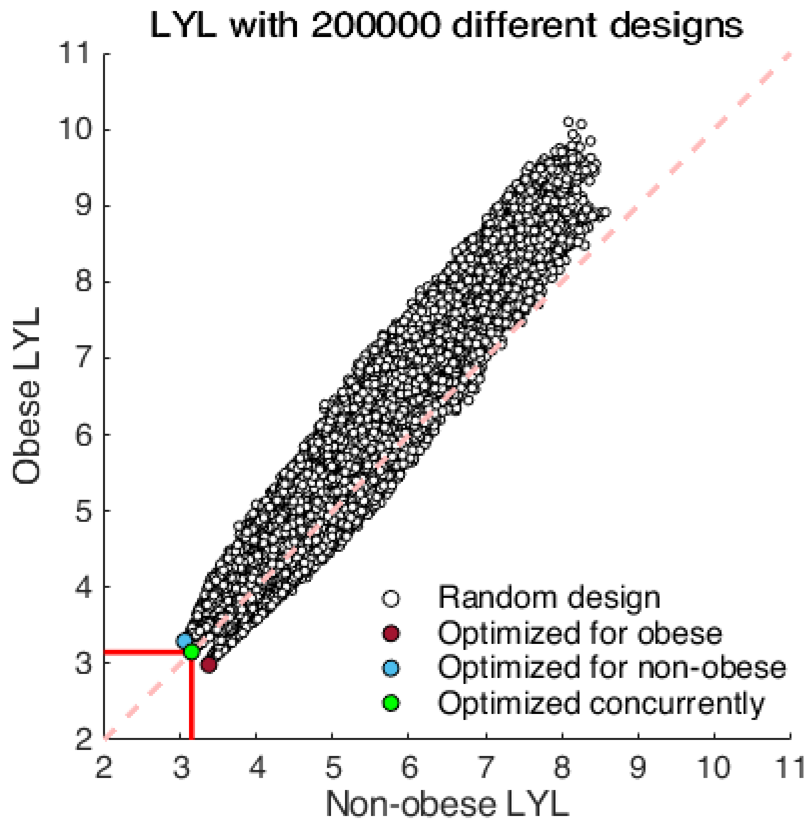

Figure 23. LYL value for the obese and non-obese HBMs with 200,000 different designs (50,000 random designs plus 150,000 designs around the optimal regions) estimated from the LYL metamodel. The inclined pink dashed line shows $y = x$ function, x and y being the horizontal and vertical axes, and the red lines represent $x + y + |x - y| = 6.3$.

Comparison to Baseline Design

The risk of injury to different body regions with both the baseline design and optimal design were below the mean values determined from the initial 450 parametric simulations. The optimal designs for obese and non-obese outperformed the baseline design in terms of LYL and risk of injury to most body regions (Figure 24). While increasing crash speed increased LYL in general, the optimum design remained more advantageous than the baseline design in speeds higher than 56 km/h. Although LYL values for both obese and non-obese HBMs were comparable with their optimized restraints in 56 km/h test, the difference in LYL between the obese HBM and the non-obese HBM grew with speed (Figure 25 and Table 10).

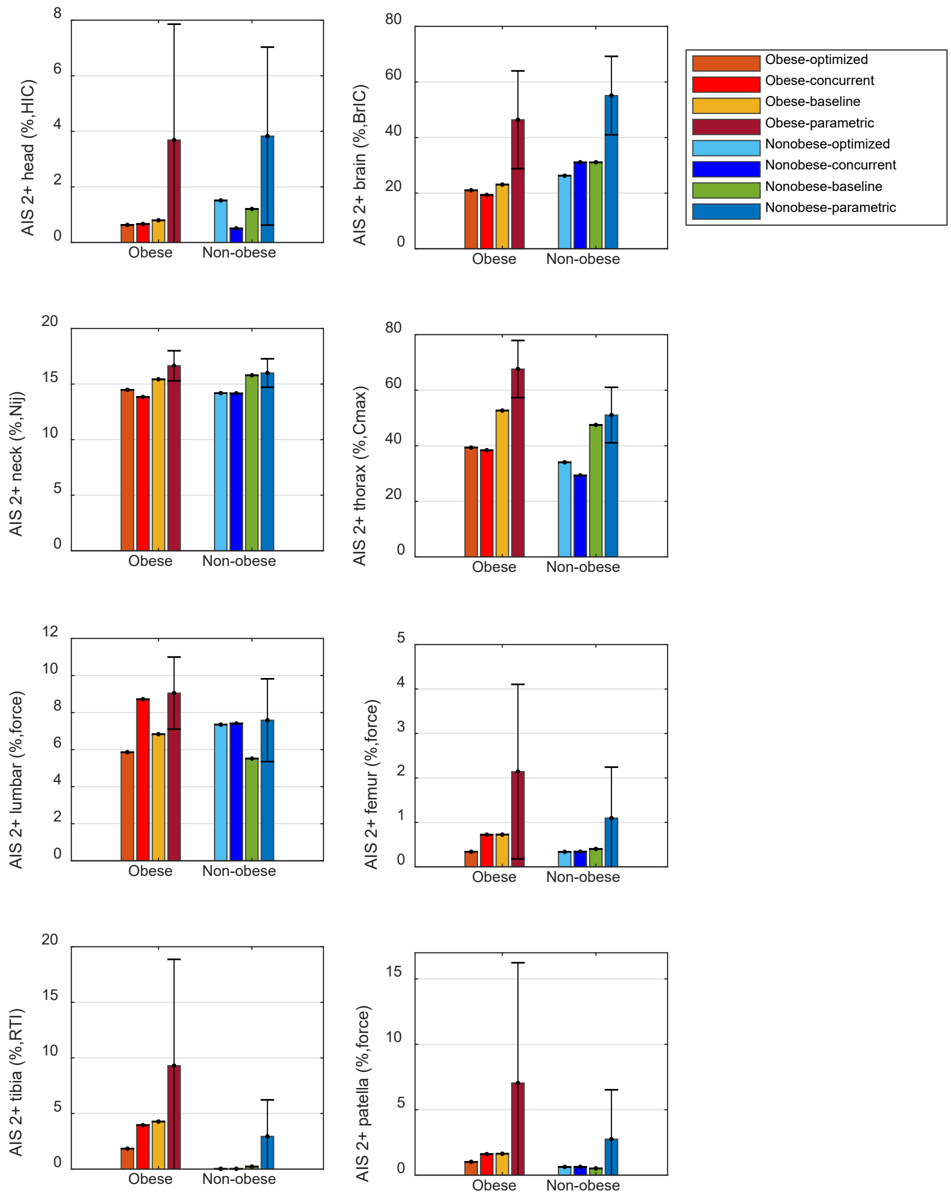

Figure 24. Risk of injury to different body regions with different restraint designs

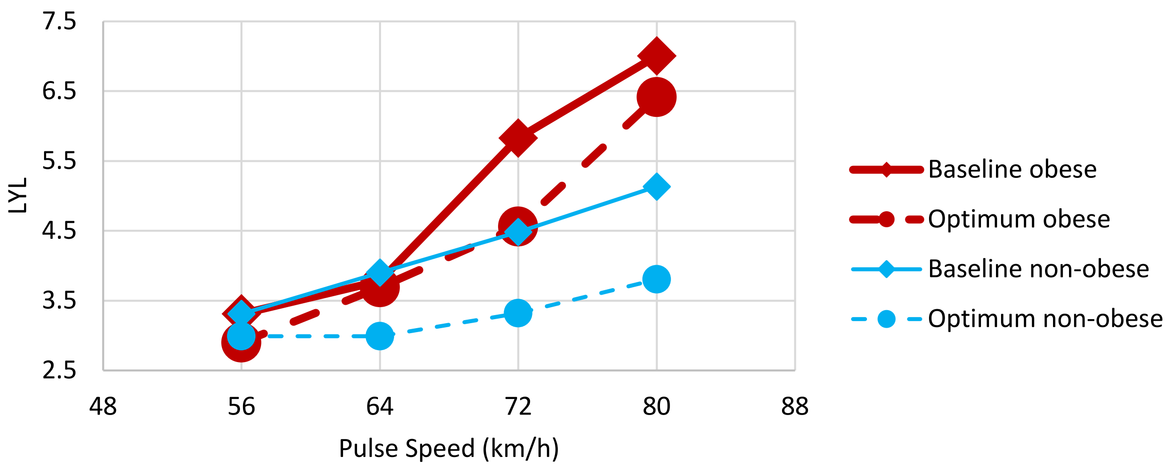

Figure 25. Comparison of LYL values at four different crash speeds with the optimized designs for obese and non-obese HBMs and baseline design

Table 10. LYL value of obese and non-obese HBMs in frontal impact tests with different speeds and a NHTSA oblique test (an average acceleration pulse from physical NHTSA oblique tests with different full-size vehicles)

	LYL value			
Test	**Baseline obese**	**Optimum obese**	**Baseline non-obese**	**Optimum non-obese**
56 km/h	3.31	2.9	3.31	2.99
64 km/h	3.78	3.69	3.9	2.99
72 km/h	5.83	4.56	4.4823	3.32
80 km/h	7.00	6.41	5.13	3.80
NHTSA oblique	4.46	3.57	4.22	4.55

Conclusions

- Overall, while the general strategy for restraining both HBMs was similar, the optimization results suggested considering the USAB as an additional countermeasure to better protect the obese HBM.
- The general restraint strategy for both occupants could include using a low LL level (e.g., 1.5 kN) to partially absorb the occupant's kinetic energy through a low force applied to the chest and a large displacement (work= force × displacement) and dissipating the remainder of this energy using other restraints including tuned DAB and collapsible steering column, which would apply the load to a wide area of the body.
- The optimized restraint for both HBMs included a low-pressure ISB, as it mitigated the risk of thoracic injury by distributing the force over a wider area compared to the standard seat belt. It also decreased the risk of neck injury by partially covering the neck.

- The optimized restraint for the obese HBM included the USAB, which made the occupant's kinematics more favorable by decreasing the lower extremity excursion and increasing the occupant's tendency to pitch forward and mitigated its lower extremity and spinal injury risk predictions. The USAB can be an effective countermeasure for increased safety of occupants with obesity.
- The findings of this study can be useful in designing adaptive restraint systems, which are effective for occupants with obesity. Adding a system to the vehicles, which can measure the occupant's weight using seat sensors and estimate the occupant's height from the seat position, may help to determine if the countermeasures, which are effective for occupants with obesity, including the USAB, should be activated during a crash.

Page intentionally left blank.

Delivered

The following were studied/provided by this work.

- The effect of obesity on the risk of injury to different body regions (Part 1)
- The most frequent injuries of occupants with and without obesity and the potential injury mechanism of the most frequent injuries of occupants with obesity (Part 1)
- Quantified comparison of the response of an obese GHBMC model to an obese PMHS, who had a similar height and BMI, in rear-seat frontal impact sled tests (Part 2)
- The effect of restraint system parameters on the obese and non-obese HBM responses, including the HBMs' kinematics and the values of different injury metrics (Part 3)
- Assessment of the prediction ability of several advanced machine learning techniques for restraint design parametric simulations (Part 4)
- Demonstrating how machine learning can be leveraged to predict the response of simulations with HBMs to avoid over-fitting and under-fitting (Part 4)
- Comparison of the parameters defining the optimized restraint system for an obese HBM, non-obese HBM, and both HBMs concurrently. It was investigated whether the obese and non-obese anthropometries required different restraint strategies (Part 5).

Page intentionally left blank.

References

Abramson, M. A. (2004). *Genetic algorithm and direct search toolbox.* The Math Works, Inc. http://cda.psych.uiuc.edu/matlab_pdf/gads_tb.pdf

Bollapragada, V. (2019). The influence of disabling injuries on the design of the vehicle front end for pedestrian safety. [Doctoral dissertation, University of Virginia].

Cormier, J., Manoogian, S., Bisplinghoff, J., Rowson, S., Santago, A. C., McNally, C., Duma, S. & Bolte, J. (2010). The tolerance of the nasal bone to blunt impact. *Annals of Advances in Automotive Medicine*, *54*, 3–14.

Cormier, J., Manoogian, S., Bisplinghoff, J., Rowson, S., Santago, A. C., McNally, C., Duma, S. & Bolte, J. (2011a). The tolerance of the frontal bone to blunt impact. *Journal of Biomechanical Engineering, 133*, 021004.

Cormier, J., Manoogian, S., Bisplinghoff, J., Rowson, S., Santago, A. C., McNally, C., Duma, S. & Bolte, J. (2011b). The tolerance of the maxilla to blunt impact. *Journal of Biomechanical Engineering, 133*, 064501.

Duma, S. M., Boggess, B. M., Crandall, J. R., & MacMahon, C. B. (2003). Injury risk function for the small female wrist in axial loading. *Accident Analysis & Prevention*, *35*(6), 869–875.

Duma, S. M., Schreiber, P., McMaster, J., Crandall, J. R., & Bass, C. (2002). Fracture tolerance of the male forearm: the effect of pronation versus supination. *Institution of Mechanical Engineers Part D: Journal of Automobile Engineering, 216*(8), 649–654. https://doi.org/10.1177/095440700221600803

Eppinger, R., Sun, E., Bandak, F., Haffner, M., Khaewpong, N., Maltese, M., Kuppa, S., Nguyen, T., Takhounts, E., Tannous, R., Zhang, A., & Saul, R. (1999, November). *Development of improved injury criteria for the assessment of advanced automotive restraint systems: II.* [Unnumbered report]. National Highway Traffic Safety Administration. www.nhtsa.gov/sites/nhtsa.gov/files/rev_criteria.pdf

Finkelstein, E. A., Chen, H., Prabhu, M., Trogdon, J. G., & Corso, P. S. (2007). The relationship between obesity and injuries among U.S. adults. *American Journal of Health Promotion*, *21*(5), 460–468.

Forman, J., Lopez-Valdes, F. J., Lessley, D., Kindig, M., Kent, R., & Bostrom, O. (2009). The effect of obesity on the restraint of automobile occupants. *Annals of Advances in Automotive Medicine*, *53*, 25–40

Funk, J. R., Crandall, J. R., Tourret, L. J., MacMahon, C. B., Bass, C. R., Patrie, J. T., Khaewpong, N., & Eeppinger, R. H. (2002a). The axial injury tolerance of the human foot/ankle complex and the effect of Achilles tension. *Journal of Biomechanical Engineering*, *124*(6), 750–757. PMID: 12596644, DOI: 10.1115/1.1514675

Funk, J. R., Srinivasan, S. C., Crandall, J. R., Khaewpong, N., Eeppinger, R. H., Jaffredo, A. S., Potier, P., & Petit, P. Y. (2002b, November). The effects of axial preload and dorsiflexion on the tolerance of the ankle/subtalar joint to dynamic inversion and eversion. *Stapp Car Crash Journal, (46)*, 245-65. doi: 10.4271/2002-22-0013. PMID: 17096228.

Hirsch, G., & Sullivan, L. (1965). Experimental knee-joint fractures a preliminary report. *Acta Orthopaedica Scandinavica*, *36*(4), 391–399. www.tandfonline.com/doi/pdf/10.3109/-17453676508988648

Hu, J., Fanta, A., Neal, M., Reed, M., & Wang, J. -T. (2016, July 21-26). *Vehicle crash simulations with morphed GHBMC human models of different stature, BMI, and age*. 4th International Digital Human Modeling Conference, Las Vegas, NE.

Joodaki, H., Gepner, B., Katagiri, M., & Kerrigan, J. (2021a, January). Evaluation of behavior of an obese human body model in frontal sled tests. *International Journal of Vehicle Safety 12*(1):15. DOI: 10.1504/IJVS.2021.115890.

Joodaki, H., Gepner, B., Katagiri, M., & Kerrigan, J. (2020a). The effects of restraint parameters on the response of an occupant with obesity: A simulation study. [Manuscript submitted for publication]. *Computer Methods in Biomechanics and Biomedical Engineering.*

Joodaki, H., Gepner, B., & Kerrigan, J. (2020b, May) Leveraging machine learning for predicting human body model response in restraint design. *Computer Methods in Biomechanics and Biomedical Engineering*, *24(*6):597-611. doi: 10.1080/10255842.2020.1841754. Epub 2020 Nov 12.

Joodaki, H., Gepner, B., Lee, S., Katagiri, M., Kim, T., & Kerrigan, J. (2021b). Is optimized restraint system for an occupant with obesity different than that for a normal BMI occupant? *Traffic Injury Prevention, 22*(8):623-628. doi: 10.1080/15389588.2021.1965131. Epub 2021 Sep 1. PMID: 34468249

Joodaki, H., Gepner, B., McMurry, T., & Kerrigan, J., (2019). Comparison of injuries of belted occupants among different BMI categories in frontal crashes. *International Journal of Obesity, 44*(6), pp.13191—132911.

Kahane, C. J. (2015). *Lives saved by vehicle safety technologies and associated Federal Motor Vehicle Safety Standards, 1960 to 2012–Passenger cars and LTVs* (Report No. DOT HS 812 069). National Highway Traffic Safety Administration. https://crashstats.nhtsa.dot.gov/Api/Public/ViewPublication/812069.pdf

Kent, R., & Patrie, J. (2005). Chest deflection tolerance to blunt anterior loading is sensitive to age but not load distribution. *Forensic Science International*, *149*(2–3), 121–128.

Kent, R., Stacey, S., Kindig, M., Woods, W., Evans, J., Rouhana, S. W., Higuchi, K., Tanji, H., Lawrence, S. S., & Arbogast, K. B. (2008, November). Biomechanical response of the pediatric abdomen, Part 2: Injuries and their correlation with engineering parameters. *Stapp Car Crash Journal, (52*), 135-66. doi: 10.4271/2008-22-0006. PMID: 19085161

Kerrigan, J. R., Drinkwater, D., Kam, C., Murphy, D., Ivarsson, B., Crandall, J., & Patrie, J. (2004). Tolerance of the human leg and thigh in dynamic latero-medial bending. *International Journal of Crashworthiness*, *9*(6), 607–623.

Kim, T., Park, G., Montesinos, S., Subit, D., Bolton, J., Overby, B., Forman, J., Crandall, J., & Kim, H. (2015, June 8-11). *Abdominal characterization test under lap belt loading*. 24th International Technical Conference on the Enhanced Safety of Vehicles, Gothenburg, Sweden.

Kim, T., Song, K., Hong, S. -H., Kim, S. -C., Choi, H. -Y., Lim, J. -M., & Shin, S. (2019, June 10-13). *A frame work to consider the new injury severity score (NISS) and a functional capacity index (FCI) in determining airbag deployment threshold*. 26th Enhanced Safety of Vehicles. Eindhovern, The Netherlands.

Kuppa, S., Wang, J., Haffner, M., & Eppinger, R. (2001, June 4-7). *Lower extremity injuries and associated injury criteria* (Paper No. 457) 17th International Technical Conference on the Enhanced Safety of Vehicles, Amsterdam, The Netherlands.

Li, C., Ford, E. S., McGuire, L. C., & Mokdad, A. H. (2007). Increasing trends in waist circumference and abdominal obesity among U.S. adults. *Obesity*, *15*(1).

Ma, X., Laud, P. W., Pintar, F., Kim, J. -E., Shih, A., Shen, W., Heymsfield, S. B., Allison, D. B., & Zhu, S. (2011). Obesity and non-fatal motor vehicle crash injuries: Sex difference effects. *International Journal of Obesity*, *35*(9), 1216–24.

Mock, C. N., Grossman, D. C., Kaufman, R. P., Mack, C. D., & Rivara, F. P. (2002). The relationship between body weight and risk of death and serious injury in motor vehicle crashes. *Accident Analysis & Prevention*, *34*(2), 221–228.

National Highway Traffic Safety Administration. (2015). New Car Assessment Program: Request for comments notice. [Docket submission, Document ID NHTSA-2015-0119 in Regulations.gov].

NCD Risk Factor Collaboration. (2016). Trends in adult body-mass index in 200 countries from 1975 to 2014: A pooled analysis of 1698 population-based measurement studies with 19.2 million participants. *The Lancet*, *387*(10026), 1377–1396. https://doi.org/10.1016/-S0140-6736(16)30054-X.

Ogden, C. L., Carroll, M. D., Kit, B. K., & Flegal, K. M. (2014). Prevalence of childhood and adult obesity in the United States, 2011-2012. *Jama*, *311*, 806–814.

Reed, M. P., Ebert-Hamilton, S. M., & Rupp, J. D. (2012). Effects of obesity on seat belt fit. *Traffic Injury Prevention*, *13*(4), 364–372.

Roberts, B. J., Thrall, E., Muller, J. A., & Bouxsein, M. L. (2010). Comparison of hip fracture risk prediction by femoral aBMD to experimentally measured factor of risk. *Bone*, *46*(3), 742–746.

Rupp, J. D., Flannagan, C. A., & Kuppa, S. M. (2010). Injury risk curves for the skeletal knee–thigh–hip complex for knee-impact loading. *Accident Analysis & Prevention*, *42*(1), 153–158.

Santago, A. C., Cormier, J. M., & Duma, S. M. (2008). Humerus fracture bending risk function for the 50th percentile male. *Biomedical Sciences Instrumentation*, *44*, 231–236.

Stemper, B. D., Yoganandan, N., Baisden, J. L., Umale, S., Shah, A. S., Shender, B. S., & Paskoff, G. R. (2015). Rate-dependent fracture characteristics of lumbar vertebral bodies. Journal of the Mechanical Behavior of Biomedical Materials, 41, 271–279.

Takhounts, E. G., Craig, M. J., Moorhouse, K., McFadden, J., & Hasija, V. (2013, November). Development of brain injury criteria (BrIC). *Stapp Car Crash Journal, (57)*, pp. 243-266

Versace, J. (1971, November 17-19). *A review of the severity index* (Report No. 710881). 15th Stapp Car Crash Conference, Coronado, CA.

Viano, D. C., Parenteau, C. S., & Edwards, M. L. (2008). Crash injury risks for obese occupants using a matched-pair analysis. *Traffic Injury Prevention*, *9*(1), 59–64.

World Health Organization. (2015). Global status report on road safety 2015. https://iris.who.int/bitstream/handle/10665/189242/9789241565066_eng.pdf?sequence=1

Zhang, Q., Kerrigan, J., Kindig, M., Arregui-Dalmases, C., & Crandall, J. R. (2013, May 19-21). *Axial injury tolerance of the clavicle and the effect of age and gender*. 9th Annual Injury Biomechanics Symposium, 1–17, The Ohio State University, Columbus, OH.

Zhu, S., Layde, P. M., Guse, C. E., Laud, P. W., Pintar, F., Nirula, R., & Hargarten, S. (2006). Obesity and risk for death due to motor vehicle crashes. *American Journal of Public Health*, *96*(4), 734–739.

DOT HS 813 540a
May 2024

U.S. Department
of Transportation

National Highway
Traffic Safety
Administration

NHTSA

16164a-050324-v3